Molecular approaches reveal speciation between red- and blue-flowered plants in the Mediterranean *Lysimachia arvensis* and *L. monelli* (Primulaceae)

FRANCISCO JAVIER JIMÉNEZ-LÓPEZ[1,2,*], JUAN VIRUEL[3,●],
MONTSERRAT ARISTA[1], PEDRO L. ORTIZ[1] and MARÍA TALAVERA[1]

[1]*Departamento de Biología Vegetal y Ecología, Facultad de Biología, Universidad de Sevilla, Apdo. 1095, 41080 Sevilla, Spain*
[2]*Phenology Lab, Biosciences Institute, Department of Biodiversity, UNESP – São Paulo State University, São Paulo, Brazil*
[3]*Royal Botanic Gardens, Kew, TW9 3DS, Richmond, UK*

Flower colour has played a decisive role as an evolutionary force in many groups of plants by driving speciation. A well-known example of colour polymorphism is found across the Mediterranean populations of *Lysimachia arvensis* and *L. monelli*, in which blue- and red-flowered plants can be found. Previous studies recognized two lineages within *L. arvensis* differing in flower colour, but this variation has not yet been considered in a phylogenetic context. We have reconstructed the ancestral states of flower colour across Mediterranean *Lysimachia* spp. aiming at understanding its phylogenetic signal using the nuclear internal transcribed spacer (ITS) sequences and three plastid markers. All blue- and red-flowered specimens were nested in different clades in the ITS tree, thus supporting that *L. arvensis* and *L. monelli* are polyphyletic, whereas low phylogenetic resolution was found in plastid markers. Monophyly was reconstructed for blue-flowered *L. arvensis* and *L. monelli* samples, and similarly for red-flowered individuals of each species: (1) blue-flowered *L. arvensis* was reconstructed as sister to the strictly blue-flowered *L. talaverae* in a monophyletic clade sister to remaining *Lysimachia*; (2) red-flowered *L. arvensis* was resolved as sister to red-flowered *L. monelli* in a monophyletic clade; and (3) clade 2 was sister to blue-flowered *L. monelli* and the strictly blue-flowered *L. foemina*. Our results suggest that colour lineages in *L. arvensis* and *L. monelli* constitute different species, but flower colour did not promote the separation of these lineages. We propose a new name for blue-flowered *L. arvensis* (*L. loeflingii*) and a new combination for red-flowered *L. monelli* (*L. collina*), maintaining *L. arvensis* for red-flowered plants and *L. monelli* for blue-flowered plants.

ADDITIONAL KEYWORDS: *Anagallis* – colour polymorphism – molecular taxonomy – nuclear and plastid DNA regions – phylogeny.

INTRODUCTION

Corolla colour is one of the most important traits influencing pollinator attraction. Different pollinators show innate preferences for specific corolla colours ([Lunau & Maier, 1995](#); [Dyer *et al.*, 2016](#)) by increasing the frequency of visits to these flowers. Petal colour polymorphism is the presence of discrete flower phenotypes genetically determined within populations of a species ([Huxley, 1955](#)). Corolla colour polymorphism

may promote speciation as it contributes to non-random mating, which can subsequently result in reproductive isolation ([Sobel & Streisfeld, 2015](#)). As a result of colour variation, species can be subject to divergent selection by pollinator preferences, and they can be subject to indirect selection resulting from genetically correlated traits (e.g. [Levin & Brack, 1995](#); [Armbruster *et al.*, 1997](#); [Armbruster, 2002](#); [Frey, 2004](#)). Indirect selection of corolla colour polymorphism, as a 'magic trait' ([Servedio *et al.*, 2011](#)), may respond to both current and palaeoclimatic abiotic factors. Historical events involved in shaping of the Mediterranean climate, such as the Messinian Salinity Crisis

*Corresponding author. E-mail: fjimenez16@us.es

(5.96–5.30 Mya; Krijgsman *et al.*, 2010) and the onset of the Mediterranean climate (3.4–2.8 Mya; Suc, 1984), have played a key role in the diversification of species (e.g. Fiz-Palacios & Valcárcel, 2013).

Lysimachia arvensis (L.) Manns & Anderb. (synonym: *Anagallis arvensis* L.) and *L. monelli* (L.) Manns & Anderb. (synonym: *Anagallis monelli* L.) are two Mediterranean species that show intraspecific flower colour polymorphism (Ferguson, 1972; Pujadas, 1997). Petal colours are genetically determined (Freyre & Griesbach, 2004; Sánchez-Cabrera *et al.*, 2021), and in both species blue- and red-flowered individuals are found due to the presence of different anthocyanins in their petals (Ishikura, 1981; Quintana *et al.*, 2008; Sánchez-Cabrera *et al.*, 2021). The species differ in ploidy, *L. arvensis* being tetraploid (revised by Pastor, 1992) and *L. monelli* being diploid (Kress, 1969; García Pérez *et al.*, 1997).

In *L. arvensis*, colour morphs also differ in other traits such as flowering phenology or type of herkogamy (Arista *et al.*, 2013; Jiménez-López *et al.*, 2020c). The colour morphs show different geographical distributional patterns, blue-flowered plants appearing mainly in drier Mediterranean localities and red-flowered plants being predominant in more temperate areas (Arista *et al.*, 2013). Blue- and red-flowered plants may appear in sympatric and allopatric populations, and pollinators show a preference for visiting blue-flowered plants in Mediterranean polymorphic populations (Ortiz *et al.*, 2015) and high colour constancy patterns (Jiménez-López *et al.*, 2020a). Hand-pollination between red and blue individuals gives rise to homogeneous F1 progeny with salmon-coloured flowers (Jiménez-López *et al.*, 2020a), but these are infrequent in wild populations (Jiménez-López *et al.*, 2020c). This 'hybrid' phenotype has been described as *Anagallis × amoena* Heldr. ex Halácsy (de Halácsy, 1904: 11). Nuclear microsatellite markers reconstructed two independent genetic groups for each colour morph, supporting this reproductive isolation between them (Jiménez-López *et al.*, 2020b). All this ecological, morphological, reproductive and molecular evidence suggests that the two colour morphs of *L. arvensis* are independent lineages.

In contrast, sympatric populations of blue- and red-flowered individuals of *L. monelli* have not been found. Blue-flowered plants are restricted to the Iberian Peninsula (Spain and Portugal), Morocco, Algeria, north-western Libya (Tripolitania) and Tunisia (Jahandiez & Maire, 1934), whereas red-flowered plants grow mainly in Morocco, Sardinia and a restricted area of Catalonia (north-eastern Spain) where blue plants were not observed (Willkomm, 1870; Jahandiez & Maire, 1934). Apart from the self-incompatibility system exhibited by the blue-flowered plants (Talavera *et al.*, 2001), little is known about

reproduction of the two morphs of *L. monelli*. A study by Quintana *et al.* (2008) found low reproductive success after hand-pollination between blue- and red-flowered plants. Nevertheless, the strikingly different geographical ranges prevent any potential crosses between blue- and red-flowered individuals of *L. monelli* in nature.

Previous phylogenetic studies have scarcely explored the potential implications of corolla colour polymorphism in taxon delimitation in *L. arvensis* and *L. monelli* because this trait was considered part of the infraspecific variation. Consequently, only one colour morph per species was sampled in most of the molecular analyses (Martins, Oberprieler & Hellwig., 2003; Manns & Anderberg, 2005, 2007a; Anderberg, Manns & Källersjö., 2007; Yan *et al.*, 2018). Only in one study (Manns & Anderberg, 2007b) was a sample from each colour morph of *L. arvensis* from a Greek locality included. These two individuals were reconstructed as a monophyletic group based on plastid markers, but were nested in independent clades in the phylogenetic tree based on internal transcribed spacer (ITS) sequences. Larger sampling of plants of the two corolla colours for both *L. arvensis* and *L. monelli* is required in phylogenetic studies to clarify the implications of flower colour in taxon boundaries. In this context, the aims of our study are to (1) investigate their phylogenetic relationships, (2) reconstruct the ancestral state of flower colour evolution, (3) suggest possible species delimitation and (4) estimate the divergence time between petal colour morphs of *L. arvensis* and *L. monelli*.

MATERIAL AND METHODS

STUDY SPECIES

Lysimachia arvensis is a Mediterranean species currently distributed across the world as an alien species. It is annual, self-compatible (Gibbs & Talavera, 2001) and tetraploid ($2x = 40$; revised by Pastor, 1992). *Lysimachia monelli* is distributed exclusively in the west of the Mediterranean Region. It is perennial, self-incompatible (Gibbs & Talavera, 2001; Talavera *et al.*, 2001) and diploid ($2x = 20$; Kress, 1969; Valdés, 1970; Šveřepová, 1972; García Pérez *et al.*, 1997).

Plant material from the other two *Lysimachia* spp. present in the Mediterranean Basin was also included (Manns & Anderberg, 2009; Aymerich & Sáez, 2015). *Lysimachia foemina* (Mill.) Manns & Anderb. is an annual, self-compatible (Marsden-Jones, 1935; Marsden-Jones & Weiss, 1938) and tetraploid species ($2x = 40$; revised by Pastor, 1992). *Lysimachia foemina*, as *L. arvensis*, is currently distributed across the world as an alien species. *Lysimachia talaverae* L.Saéz & Aymerich (Aymerich & Sáez, 2015) is

endemic to the western Mediterranean, and is annual, self-compatible (Gibbs & Talavera, 2001) and diploid (2*x* = 20; Šveřepová, 1972; García Pérez *et al.*, 1997).

MOLECULAR SAMPLING, DNA EXTRACTION, PCR AMPLIFICATION, SEQUENCING AND ALIGNMENT

Fresh leaf material from 28 populations of *L. arvensis* (LA), 12 of *L. monelli* (LM), three of *L. foemina* (LF) and four of *L. talaverae* (LT) (Fig. 1; Supporting Information, Table S1) was collected and dried in silica-gel (Chase & Hills, 1991). This sampling represents nine pure red and 12 pure blue populations and seven mixed (red and blue) populations of *L. arvensis* (the colour of each sample was coded as LA_R for red-flowered samples and LA_B for blue-flowered samples in *L. arvensis*). Sampling of *L. monelli* included four pure red (LM_R) and eight pure blue populations (LM_B). Also, one sample of *L. azorica* Hornem. ex Hook. (LZ) and one sample of two populations of *L. linum-stellatum* (L) Hoffmanns. & Link were included (Table S1) in the phylogenetic analyses, and *L. tenella* L. (AY855150) and *L. tyrrhenia* U.Manns & Anderb. (AY855136) were used as outgroups.

Total genomic DNA was isolated with Invisorb Vegetal DNA Kit HTS 96 (Invitek, Spain), with modifications following Jiménez-López *et al.* (2016). The quality of the extracted DNAs was checked in a 1% TAE-agarose gel, and DNA concentration was estimated using a NanoDrop DS-11 Spectrophotometer (DeNovix).

The nuclear ribosomal DNA (nrDNA) ITS and three plastid markers were used for phylogenetic reconstructions. The partial 18S, ITS-1, 5.8S, ITS-2 and partial 28S regions of the rDNA were amplified using primers ITS5 and ITS4 (White *et al.*, 1990). We tested 19 plastid markers (Supporting Information, Table S2) in eight samples of *L. arvensis* (four blue and four red specimens), but only three of them showed polymorphic sites between samples. PCR amplifications of ITS were performed following Jiménez-López *et al.* (2016) using 4 ng of DNA as input, and the polymorphic plastid markers *rps16-trnK* and *rpl32-trnL* were amplified following Shaw *et al.* (2007) and *trnH-psbA* was amplified following Hamilton (1999). After purification with ExoSAP-IT (Roche, Spain), fragments were sequenced in an ABI 3730 machine using the BigDye Terminator Cycle Sequencing Kit (Applied Biosystems, Foster City, CA, USA) at STAB Vida Lda. (Oeiras, Portugal).

Both forward and reverse DNA sequences were obtained and assembled from double-stranded PCR products. The ITS sequences were carefully checked for double peaks. Twelve bases proved to have polymorphic states in some taxa, probably due to incomplete homogenization between different ITS paralogues. Eight of these bases, present in more than one sample, never in different taxa, were removed before analysis to avoid artificial results, following Manns & Anderberg (2007b). Sequences were edited using Geneious R10 (Biomatters Ltd, Auckland, New Zealand) and the ends of each sequence, of low quality, were trimmed. Alignments were conducted in MEGA v.X (Kumar *et al.*, 2018; Stecher, Tamura & Kumar, 2020) using the algorithm Clustal W (Thompson, Gibson & Higgins, 2002), and visually inspected. Four insertions/deletions (indels) of single bases were identified for the ingroup in the ITS matrix, and seven indels separated ingroup
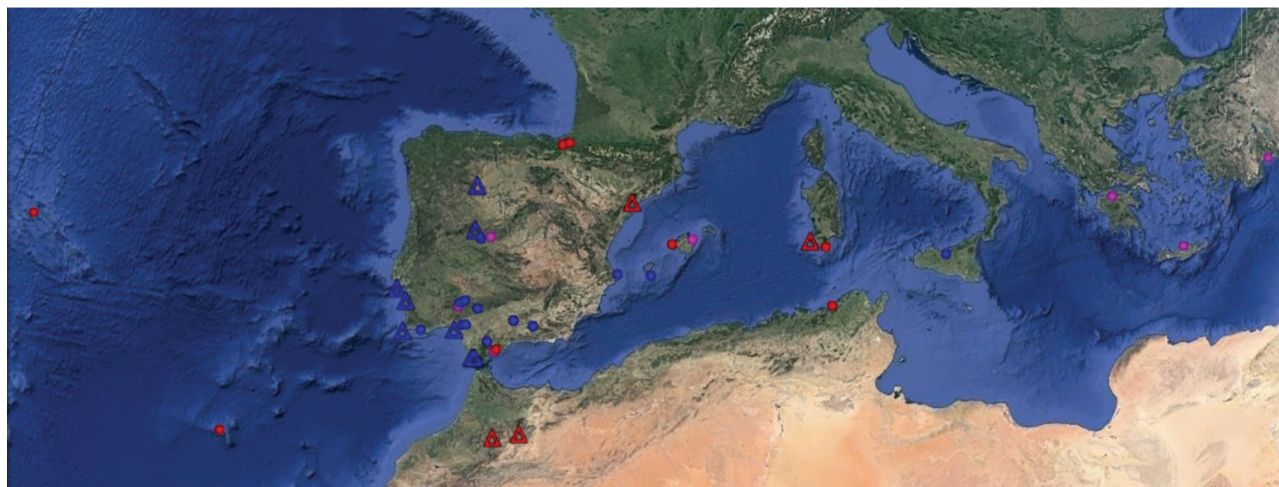

Figure 1. Geographical distribution of the studied populations of *Lysimachia arvensis* (circles) and *L. monelli* (triangles). Colours correspond to flower colour of the studied populations: blue and red for pure blue and red populations, respectively, and pink for mixed populations. Map based on the projection generated by Google Earth for the coordinates of the studied populations (Table S1).

taxa from outgroups; there were four indels (1–4 bp long) in ITS1 and three indels (4–7 bp long) in ITS2. Indels in the ITS matrix were coded as gaps and treated as partial deletions. In the plastid DNA regions, five indels were identified within the ingroup. Two indels (one of 4 bp and other of 1 bp) in the *rps16-trnK* matrix, two (1 bp) in the *rpl32-trnL* matrix and one (1 bp) in the *trnH-psbA* matrix were present. However, the outgroup showed 21 indels for the three plastid DNA regions studied: 11 in the *rps16-trnK* matrix (1–20 bp long), four in the *rpl32-trnL* matrix (5–9 bp long) and five in the *trnH-psbA* matrix (1–7 bp long). These indels were coded as gaps and treated as partial deletions. Finally, in the *trnH-psbA* matrix, one long insertion (69 bp) was observed in the outgroup with respect to the ingroup, which was excluded from the analysis.

PHYLOGENETIC INFERENCE

The Akaike information criterion (AIC) was used to estimate the evolution model that better fits each DNA matrix using jModeltest 2.1.4 (Darriba *et al.*, 2012). Phylogenetic relationships were inferred based on maximum-parsimony (MP) inference using PAUP* (Swofford, 2003) and maximum-likelihood (ML) methods using RAxML v.8 (Stamatakis, 2014). Bootstrap support (BS) was estimated with 1000 bootstrap replicates following full heuristic searches. Bayesian inference (BI) was conducted using MrBayes (Ronquist *et al.*, 2012) on X_{SEDE} (3.2.7a) (CIPRES Science Gateway v,3.3; Miller, Pfeiffer & Schwartz, 2010). Phylogenetic reconstructions were calculated for each DNA region (ITS and each of the three plastid DNA markers), and for a concatenated matrix of the three plastid regions. Following Viruel *et al.* (2016), clades with BS of 75–100 or posterior probability (PPS) of 0.95–1.0 were considered moderately to strongly supported. Phylogenetic reconstruction with ITS was performed with and without the sample LA19_B according to the results of the recombination analysis (see below and Results).

To test for incongruent topologies between the independent DNA data matrices, a partition homogeneity test was performed (Farris *et al.*, 1994; Symonds & Lloyd, 2003). The incongruence length difference (ILD) test of Farris *et al.* (1994) implemented in PAUP* (Swofford, 2003) was performed using 1000 random-order-entry replicates to estimate if the nuclear and the three plastid data sets were significantly different from random partitions of the same size.

RECOMBINATION ANALYSIS

To test possible recombination events in the ITS sequences of all the samples, seven methods (RDP, GENECONV, BootScan, MaxChi, Chimaera, SiScan and 3SEQ) implemented in RDP4 v.484 were applied to infer recombination events (Martin *et al.*, 2015; Viruel *et al.*, 2018).

ANCESTRAL STATE RECONSTRUCTION

To estimate the ancestral state of flower colour, we performed ancestral state reconstruction of colour classes using an ML approach with the function 'ace' and a Markov chain Monte Carlo (MCMC) approach called stochastic character mapping (SIMMAP; Huelsenbeck *et al.*, 2003) included in the package 'phytools' (Revell, 2012) implemented in R. We performed the analyses on the RAxML phylogenetic tree obtained from the ITS dataset. We fitted three different models for both approaches (ML and SIMMAP): equal-rate model (ER), symmetric model (SYM) and all-rate-different model (ARD). The best-fitting model was selected according to the AIC. For SIMMAP analyses, we ran 1000 simulations per tree. Because we included more than one sample per species, we also pruned the additional samples for the same species in the case of monophyly. Ancestral state reconstruction was shown only on major clades.

SPECIES DELIMITATION

Putative species limits were explored with four methods: (1) a multi-rate Poisson tree process (mPTP) provided at the mPTP webpage (https://mptp.h-its.org) (Kapli *et al.*, 2017); (2) the Automatic Barcode Gap Discovery (ABGD) (Puillandre *et al.*, 2012); (3) a 'classical' DNA barcoding gap analysis based on the Kimura two-parameter (K2P) method (Kimura, 1980) assessed with the APE R package (Paradis, Claude & Strimmer., 2004) and ggplot2 R package (Wickham, 2011); and (4) the species delimitation plugin (SDP) (Masters, Fan & Ross., 2011) implemented in Geneious. These methods were applied to the ITS sequence data, commonly used for inferring phylogenetic relationships at low taxonomic levels (Soltis & Soltis, 1998; Duminil & Di Michele, 2009). The mPTP inferred putative species boundaries on an ML phylogenetic input tree, assigning intra- or interspecific categories of each branch. The multi-rate implementation of the mPTP considers different evolutionary rates in the differentiation of each putative species and uses a single ML tree as input. To run the mPTP model on our dataset, we uploaded the previously estimated RAxML tree, following Hanusch *et al.* (2020). The K2P model estimated evolutionary divergence between sequences from the average number of base substitutions per site of all sequence pairs among groups, with a gamma distribution; and standard error estimates were obtained by a bootstrap procedure (100 replicates). The ABGD method statistically infers and finds the

distance at which a barcode gap occurs and sorts the sequences into molecular operational taxonomic units (MOTUs) based on this distance (Puillandre *et al.*, 2012). ABGD was run online (https://bioinfo.mnhn.fr/abi/public/abgd/abgdweb.html) with default settings [Pmin = 0.001, Pmax = 0.1, Steps = 10, X (relative gap width):1.5 & Nb bins (for distance distribution): 20] and with Kimura (K80) TS/TV distances (Kimura, 1980). Finally, the SDP in the Geneious software evaluates the phylogenetic monophyly of each putative taxon considered as a clade by testing the probability that this monophyly occurred in a coalescent process, and it assesses the probability with which a putative taxon can be diagnosed successfully on a phylogenetic tree by comparing intra- and interspecific genetic distances (Masters *et al.* 2011). SDP was used to calculate intra/inter ratios ('intra' is the differentiation among members of a clade, and 'inter' is the genetic differentiation between the members of a clade and its closest neighbouring clade), values of P ID(Strict) (the mean probability that an unknown specimen of a given clade will effectively be placed within this clade), and two statistical tests: Rosenberg's P_{AB} (Rosenberg, 2007) and Rodrigo's P (PD) (Rodrigo *et al.*, 2008). Rosenberg's P_{AB} tests whether the monophyly of the selected group in the gene tree is due to an evolutionary process or if it is the result of random branching of the tree caused by an insufficient sample size (Rosenberg, 2007). Rodrigo's P (Randomly Distinct) uses the ratio between the length of the branches within a selected group and the length between selected groups to estimate whether the distinctiveness of the groups is due to an evolutionary process or to random coalescent processes (Rodrigo *et al.*, 2008).

DIVERGENCE-TIME ESTIMATION

We used molecular clock approaches to estimate divergence times among the main clades. We selected one random sequence for each colour and taxon studied, with sequences of other *Lysimachia* and related species from GenBank (Supporting Information, Tables S1 and S3). A phylogenetic reconstruction was inferred with ML methods with RAxML (Stamatakis, 2014) following the parameters described above. We used a Bayesian uncorrelated-lognormal relaxed-clock approach (Drummond *et al.*, 2006) as implemented in BEAST v.2.5 (Bouckaert *et al.*, 2019). Node ages and absolute branch substitution rates were estimated using two relaxed clock methods that represent two contrasting approaches to estimate divergence times (Magallón, Hilu & Quandt, 2013). We used both Yule speciation and birth–death tree priors (Heled & Drummond, 2012). We ran 30 independent analyses (50 million generations each, sampled every 5000

generations). Tracer 1.7.1 software (Rambaut *et al.*, 2018) was used for convergence and satisfactory effective sample size (ESS) values (> 200) and verify that a burn-in of 10% was appropriate. Subsequent parameter distributions were obtained by combining the independent MCMCs with LogCombiner 1.10.4 and calculating the maximum credibility tree using TreeAnnotator 1.10.4 (Suchard *et al.*, 2018).

Fossil records are scarce because these plants lack woody parts, and both seed and pollen production are low. *Maesa* Forssk is a first-diverging taxon in Primulaceae (Anderberg *et al.*, 2007; Yesson, Toomey & Culham, 2009) and its pollen is known from the Early Eocene (55.8 Mya; Huzioka & Takahasi, 1970) according to the Paleobiology Database (http://paleodb.org/). Furthermore, fossil seeds similar to those of *Lysimachia vulgaris* L. and its close relatives (Oh *et al.*, 2008) are found from the Mid-Miocene (12–16 Mya; Friis, 1985). We therefore used the pollen record to set the age prior for rooting and seed fossil to set the age prior for *L. vulgaris*. The most generally appropriate prior for fossil calibrations is the lognormal distribution (Ho & Phillips, 2009). In addition, a secondary calibration was applied to the stem age of core *Lysimachia* L. using an estimated mean age of 30 Mya from previous phylogenetic reconstructions (Yesson *et al.*, 2009; Zanne *et al.*, 2014). In this case, we used a standard normal prior distribution with mean of 30 Mya and standard deviation (SD) of 6 Mya, yielding a 95% highest posterior density (HPD) of 20–40 Mya, following Yan *et al.* (2018). To test the effect of different calibration points and tree prior approaches, we also performed analyses using only one fossil calibration, only secondary calibration and both calibration points. We then performed a regression between the node ages of the same clades from all analyses.

RESULTS

PHYLOGENETIC RECONSTRUCTIONS

Fifty-two high-quality sequences were obtained for ITS, and 37 for the plastid regions. The ITS1 and ITS2 fragments in the ingroup alignment ranged from 230 to 231 and 205 to 207 bp, respectively. No significant variation among samples within each taxon was found, except six samples of LA_B (LA4_B, LA6_B, LA7_B, LA11_B, LA12_B & LA13_B), which showed three consistent transitions of 1 bp (two in ITS1 and one in ITS2) with respect to the other LA_B samples. A total of 625 aligned characters of ITS sequences were used for phylogenetic analyses. We observed 406 constant characters (65.0%), 27 variable parsimony-uninformative characters (4.3%) and 192 potentially parsimony-informative characters (30.7%). The

heuristic search resulted in six MP trees, with a tree length (TL) of 304, a consistency index (CI) of 0.84 (excluding uninformative characters) and a retention index (RI) of 0.94.

The ILD test showed significant differences between nuclear and plastid regions ($P = 0.010$), indicating inconsistency between these markers. Thus, phylogenetic analyses were performed for the ITS region separately from the concatenated dataset representing the three plastid markers.

The MP, RAxML and Bayesian trees reconstructed the same topology for all analyses based on the ITS region (Fig. 2). Two main clades were observed:

Clade I (C1, 62 BS, 0.9988 PPS) which contained LA_B samples (100 BS, 1.000 PPS) sister to LT (97 BS, 1.000 PPS), whereas the samples of *L. arvensis* from south-west Spain (LA4_B, LA6_B, LA7_B and LA11_B-LA13_B) formed a clade (82 BS, 0.975 PPS); and Clade II (C2; 80 BS, 0.850 PPS) comprising two subclades, named A and B. In subclade A (SCA; 87 BS, 0.968), LA_R samples (95 BS, 1.000 PPS) were sister to the LM_R samples (100 BS, 1.000 PPS). In subclade B (SCB; 94 BS, 0.9859), LM_B samples (99 BS, 0.999 PPS) were sister to LF (100 BS, 1.000 PPS). Therefore, blue and red individuals of both *L. arvensis* and *L. monelli* appeared in different groups. Blue- and
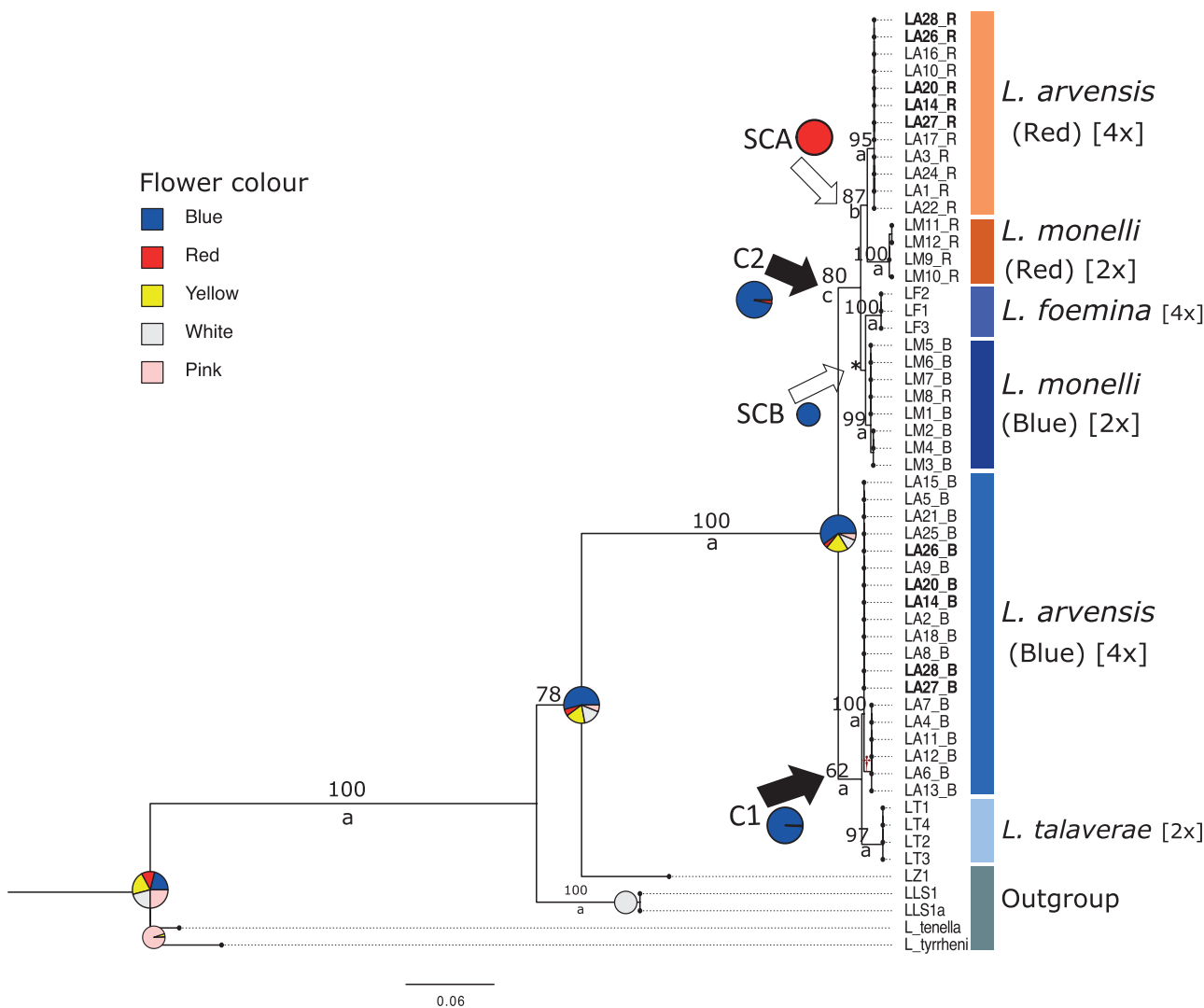
Figure 2. Ancestral state reconstruction of flower colour of *Lysimachia arvensis*, *L. monelli* and related taxa (see Table 1). RAxML tree based on ITS sequences. The samples of *L. arvensis* from mixed populations are highlighted in bold. Bootstrap values > 50% are given above the branches. Posterior probabilities of the Bayesian approach were coded as: a (0.995–1.000 PPS), b (0.950–0.994 PPS) and c (0.850–0.949); these are indicated below branches. C1: Clade 1; C2: Clade 2; SCA: Subclade A and SCB: Subclade B. * (94 BS, 0.9859 PPS); † (82 BS, 0.975 PPS).

red-flowered individuals from mixed populations of *L. arvensis* appeared in independent clades (Fig. 2; Supporting Information, Fig. S1).

Each plastid DNA partition (*rps16-trnK*, *rpl32-trnL* and *trnH-psbA*) varied on aligned length, number of potentially informative sites and values of parsimony analyses (Table 1). Visual analysis of these sequences pointed to a split in two main haplotypes, particularly in the *rps16-trnK* and *rpl32-trnL* matrices. All LT and LA_R, and most LA_B samples share one haplotype (H1), whereas LM_B, LM_R, LF and some LA_B samples share another haplotype (H2). Both haplotypes are differentiated by the presence of indels and several single base mutations (Table 2), and H1 is more divergent from the outgroup than H2. For each plastid DNA region separately, the trees reconstructed showed a congruent topology in all analyses and markers (Supporting Information, Figs S2–S4). The concatenated plastid DNA dataset comprised 1695 aligned characters, of which 1459 were constant characters (86.1%), 159 variable parsimony-uninformative characters (9.4%) and 77 potentially parsimony-informative characters (4.5%). Heuristic search resulted in 100 MP trees, with a TL of 129, CI of 1.0 (excluding uninformative characters) and RI of 1.0. The phylogenetic tree reconstructed with the concatenated plastid DNA matrix showed two clades (Fig. 3; Fig. S5). The first clade (94 BS, 1.000 PPS) comprised all the red- and some blue-flowered individuals of LA and LT. The second clade (86 BS, 0.890 PPS) included blue-flowered individuals of LA, LM (blue and red) and LF. Concordant results with the two haplotypes were observed visually. This topology was also observed for each plastid marker independently, although the bootstrap support was lower in all cases (Figs S2–S4).

RECOMBINATION ANALYSES

No recombination events were invoked across samples, except for a blue-flowered *L. arvensis*

Table 1. Aligned information, parsimony analysis results and evolutionary model used for each plastid DNA partition

	rps16-trnK	*rpl32-trnL*	*trnH-psbA*
Aligned base pairs	711–715	609–611	373
Potentially informative characters	18	14	9
MP trees/tree length	1/61	10/35	1/32
Consistency index	0.97	0.97	0.93
Retention index	0.96	0.98	0.71
Evolutionary model	GTR	TrN	HKY

(LA19_B), in which four of the seven recombination methods detected two recombinant regions of 18 nucleotides starting at position 16 from *L. arvensis* and of 25 nucleotides starting at position 133 from *L. foemina*. Therefore, this sample was excluded from the phylogenetic tree shown in Figure 2, but it is shown in Supporting Information, Figure S1.

ANCESTRAL STATE RECONSTRUCTION

The ER model was the best-fitting model according to AIC both for ML (AIC ER: 0.99956394, SYM: 0.00043601 and ARD: 0.00000005) and for SIMMAP (AIC ER: 0.99956397, SYM: 0.00043601 and ARD: 0.00000002) analysis. Both approaches showed the same evolutionary transition of flower colour: a high probability of blue-flowered plants until the ancestor of the SCA clade, when red-flowered plants probably appeared (Fig. 2).

SPECIES DELIMITATION

The ITS phylogenetic reconstructions pointed to six MOTUs (LA_R, LM_R, LF, LM_B, LA_B and LT), which were consistent with the characterized indel positions (Table 2) and with the evolutionary divergence between samples estimated by the K2P model. Mean p-distances between the six MOTUs ranged from 0.0143 to 0.0622 and within each MOTU from 0.0000 to 0.0023 (Table 3).

In addition, three of the four methods applied for species delimitation confirmed these clusters. Only the mPTP model differed by identifying an additional MOTU resulting from dividing LA_B in two: one with LA4_B, LA6_B, LA7_B, LA11_B, LA12_B and LA13_B (blue-flowered samples from populations of south-western Spain), and one with the rest of the LA_B samples.

The ABGD method was run with a prior maximum divergence of intraspecific diversity. The number of groups for the recursive partition was six with a prior of 0.008; seven with 0.005 and 0.003; and nine with 0.001. The primary partition was stable on the range of prior values, with six groups corresponding to the same groups obtained with a prior of 0.1.

The same groups were supported by DNA barcoding gap analysis. Heat-map analysis showed that sequence dissimilarity was < 1 within each MOTU and 1–5 between samples of different MOTUs (Fig. 4). DNA barcoding gap analysis showed no overlap between intra- and interspecific distances among MOTUs (Fig. 4). Indeed, intraspecific genetic distances were close to 0 within each MOTU, whereas interspecific genetic distances ranged from 0.010 to 0.050 between MOTUs/species (Supporting Information, Fig. S6).

Table 2. Summary of sequence variation in the nuclear ribosomal DNA regions (ITS 1 and ITS2) and plastid DNA partitions (*rps16-trnK*, *rpl32-trnL* and *trnH-psbA*) in the ingroup of the studied *Lysimachia* species

	ITS1																ITS2													
Site	14	29	46	49	56	57	116	119	120	121	122	123	128	167	195	196	420	421	422	437	442	476	477	478	527	548	564	565	574	591
Type of change:																	Del		Ins						Del					
Consensus:	T	T	C	G	C	G	G	C	G	C	A	T	C	A	T	C	C	A	-	C	G	C	T	A	G	T	C	C	C	C
LA_B	A	*	*	*	*	*	*	*	*	*	*	*	*	*	*	*	*	*	*	*	T	G	A	*	*	A	*	A	*	*
LA_B (2)†	A	*	T	*	T	*	*	*	*	*	*	*	T	T	*	*	*	*	*	*	T	G	A	*	*	A	T	A	T	*
LA_R	*	C	*	A	*	*	A	T	C	G	T	G	*	*	*	*	-	C	A	T	*	*	*	C	-	*	*	*	*	*
LF	*	C	*	*	*	*	T	T	A	T	C	C	*	*	*	*	*	C	*	*	*	*	*	*	-	*	*	*	*	*
LM_B	*	C	*	*	*	*	C	*	A	T	C	C	*	*	A	*	*	*	*	*	*	*	*	*	*	*	*	*	*	T
LM_B (2)‡	*	C	*	*	*	*	C	*	A	T	C	A	*	*	A	*	*	*	*	*	*	*	*	C	*	*	*	*	*	T
LM_R	*	C	*	*	*	*	C	*	C	G	T	G	*	*	*	G	*	*	*	*	*	*	*	*	*	*	*	*	*	A
LT	*	*	*	*	*	A	*	*	*	*	*	C	*	T	*	*	*	*	*	*	T	G	A	*	*	A	*	*	A	*

	rps16-trnK											*rpl32-trnL*							*trnH-psbA*		
Site	113	424	467	468	471	472	473	474	475	498	589	59	173	176	188	333	342	584	40	360	365
Type of change				del	del	del	del	del	del	del	del					Ins	Ins			Del	
Consensus	T	A	G	A	A	G	—	—	—	G	—	G	T	T	T	—	—	G	T	G	—
H1	*	*	*	*G¹	—	—	—	—	—	G	—	*	*	*	—	*	*	*	G	*	*
H2	G	G	A	A	A	A	A	A	A	A	T	T	*C²	C	G	T	*T¹	G	C	A	G

Del: deletion; Ins: insertion.

†(LA4_B, LA6_B, LA7_B, LA11_B- LA13_B).

‡(LM3_B-LM5_B; see Supporting Information, Table S1).

Haplotype 1 (H1)/Haplotype 2 (H2) comprise the clade 1/clade 2 samples of the concatenated plastid DNA tree (Fig. 3).

1, only on LF and LM_B samples of H2; 2, only on LA_B samples of H2; Fig. 3, Table S1).
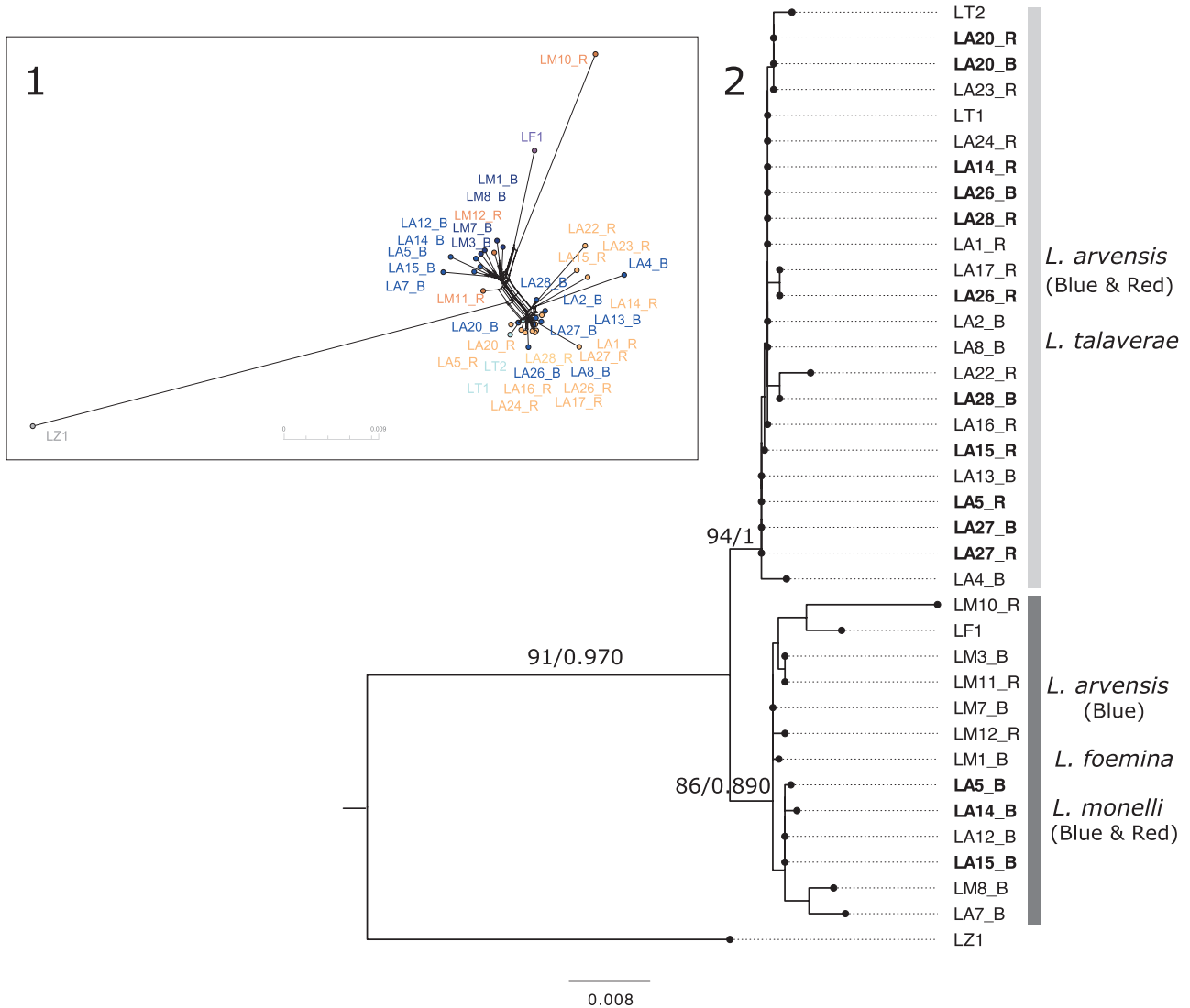
Figure 3. Phylogenetic network (1) and maximum-likelihood (ML) (RAxML) (2) tree based on concatenated plastid sequence data (*trnH-psbA*, *rps16-trnK* and *rpl32-trnL*) of *Lysimachia arvensis*, *L. monelli* and related taxa (see Table 1). Main clades in trees from ML (RAxML) and Bayesian analysis (MrBayes) are identical. Bootstrap values > 50% and posterior probabilities of the Bayesian approach (BS/PPS) are given above the branches. Samples of *L. arvensis* from mixed populations are highlighted in bold.

Finally, the results of the SDP also suggest six MOTUs/species for both BI and ML approaches, particularly with Rosenberg's P_{AB} statistics (Table 4). In general, the six initial MOTUs/species were monophyletic. For both BI and ML, most Intra/Inter ratios were < 1, indicating that the divergence within each MOTU was low relative to the divergence with the closest MOTU. Values of P ID(Strict) in BI were higher for MOTUs LA_B and LA_R than for the remaining MOTUs, and hence were correctly identified. Rosenberg's P(AB) values were significant ($P < 0.05$) for all MOTUs/species in the BI and ML

trees. However, Rodrigo's P(RD) values were significant ($P < 0.05$) for all MOTUs/species only in the BI tree.

DIVERGENCE TIME ESTIMATION

Similar time estimates and topologies were obtained using the three different calibration ages and different tree priors for the stem age of tribe Lysimachieae (Fig. 5; Supporting Information, Fig. S7). Divergence time results based on these different strategies were all similar to each other (Table S4). Our primary analyses (Fig. 5) used the full tree with the Yule prior and all

Table 3. Mean p-distances and their standard errors between and within (diagonal) the different MOTUs: *Lysimachia arvensis* (LA), *L. monelli* (LM), *L. foemina* (LF) and *L. talaverae* (LT); blue- (B) and red-flowered (R) samples based on the ITS data estimated with the K2P model

MOTU	LA_R	LM_R	LF	LM_B	LA_B	LT	outgroup
LA_R	0.0000 ± 0.0000						
LM_R	0.0184 ± 0.0047	0.0020 ± 0.0014					
LF	0.0225 ± 0.0070	0.0271 ± 0.0076	0.0000 ± 0.0000				
LM_B	0.0144 ± 0.0053	0.0243 ± 0.0065	0.0143 ± 0.0049	0.0009 ± 0.0010			
LA_B	0.0400 ± 0.0080	0.0519 ± 0.0133	0.0453 ± 0.0078	0.0388 ± 0.0077	0.0023 ± 0.0012		
LT	0.0510 ± 0.0098	0.0622 ± 0.0170	0.0563 ± 0.0098	0.0498 ± 0.0095	0.0170 ± 0.0053	0.0000 ± 0.0000	
outgroup	0.3214 ± 0.0745	0.3149 ± 0.0732	0.3227 ± 0.0773	0.3196 ± 0.0743	0.3232 ± 0.0791	0.3359 ± 0.0791	0.2095 ± 0.0451

MOTUs were defined by Species Delimitation plugin (SDP) Bayesian inference (BI) analysis.

calibration points. The correlation between the node ages of clades from the primary tree and alternative trees based on different calibration schemes and tree priors were significant for all cases (r^2 = 0.926–0.974, P < 0.001; see Table S5). The maximum clade credibility (MCC) tree of Lysimachieae showed three clades in *Lysimachia* (Fig. 5): one with *L. arvensis*, *L. monelli* and related species (BS 100%; 1.000 PPS, Clade A); one with *L. vulgaris*, *L. punctata* L. and related species (0.940 PPS, Clade B); and one with *L. tenella*, *L. minima* (L.) U.Manns & Anderb. and other related species (BS 100%; 0.990 PPS, Clade C). The last clade appeared closest to species of *Cyclamen* L. (BS 100%; 1.000 PPS). According to the relaxed molecular clock and Yule tree priors, the common ancestor of blue-flowered plants of *L. arvensis* and *L. talaverae* diverged *c*. 2.4 Mya (95% HPD 0.5–4.1), the divergence of blue-flowered plants of *L. monelli* and *L. foemina* probably occurred *c*. 1.0 Mya (95% HPD 0.3–2.0), and the split between red plants of *L. arvensis* and red plants of *L. monelli* was estimated at *c*. 1.7 Mya (95% HPD 0.5–2.5). Furthermore, the common ancestor between LA_R-LM_R and LM_B-LF subclades probably diverged *c*. 2.1 Mya (95% HPD 1.0–3.5) and the divergence between these clades and LA_B-LT clade occurred *c*. 5.2 Mya (95% HPD 2.9–8.1) (Fig. 5; Fig. S7). Two divergence events occurred during the Miocene between the different clades of *Lysimachia*. The first one happened *c*. 33.5 Mya (95% HPD 28.4–40.4), the split of clade C from the other *Lysimachia* clades, and the second one happened *c*. 29.9 Mya (95% HPD 24.8–36.9) dividing clades A and B (Fig. 5; Fig. S7).

DISCUSSION

SPECIES BOUNDARIES IN THE MEDITERRANEAN *LYSIMACHIA*

Our phylogenetic results based on nuclear ITS regions indicate that blue- and red-flowered individuals of *L. arvensis* and *L. monelli* are independent taxa (Fig. 2), reinforcing ecological, morphological and reproductive evidence. The results of the present study could accommodate the genealogical concept of species, in which all alleles of a given gene are descended from a common ancestral allele not shared with those of other species (Baum *et al.*, 1995). Although the presence of different ITS sequences in the red- and blue-flowered individuals of *L. arvensis* collected from the same populations had already been reported by Manns & Anderberg (2007b), the strong support of our ITS (100 BS, 0.999 PPS) and the species delimitation results (Table 4, Fig. 5) indicate that the two colour morphs of *L. arvensis* are different lineages and belong to different taxa. The ITS phylogenetic reconstruction
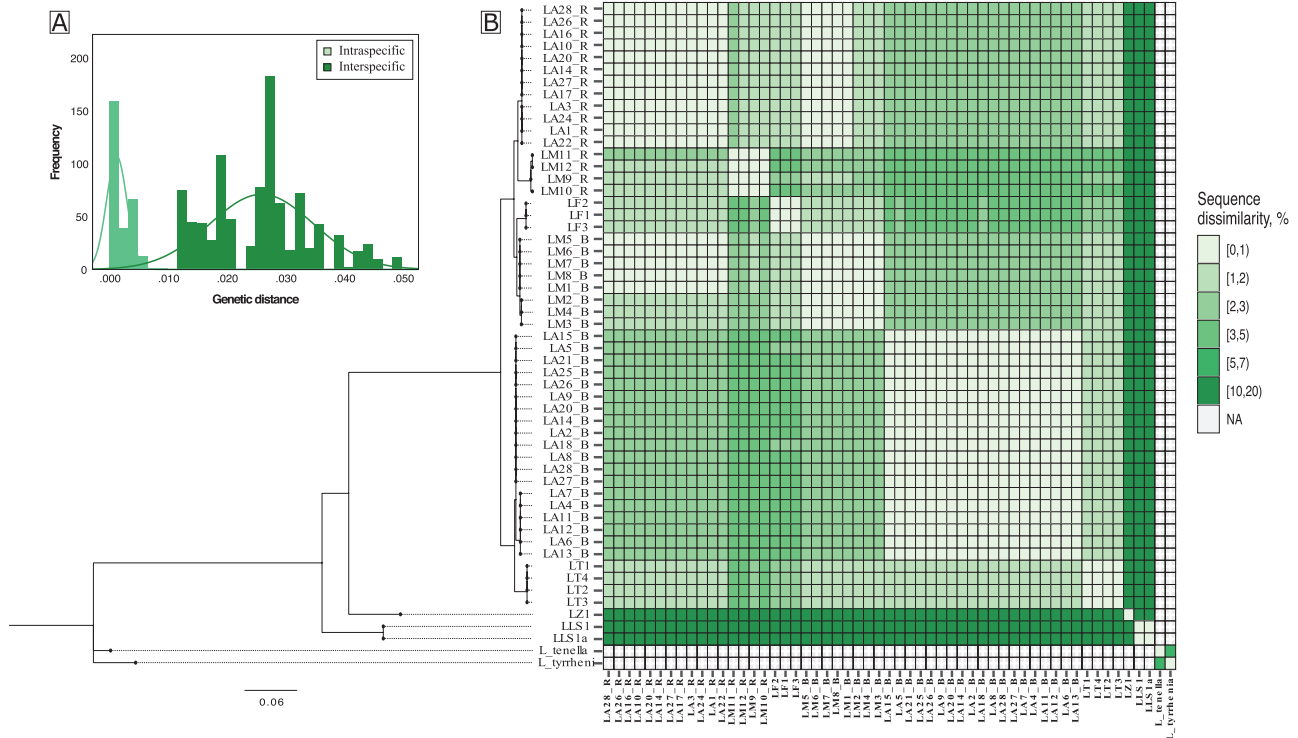
Figure 4. Intra-/interspecific genetic distance plot (A) and heatmap representing genetic dissimilarity (B) based on ITS sequences of the studied *Lysimachia* species. A, genetic distance between samples of the DNA barcoding gap analysis based on the K2P method. MOTUs of SDP BI analyses (Table 4) were considered to define intra-/interspecific categories. B, dissimilarity distances between sequences, as simply the proportion of sites (%) that differ between each pair of sequences, were assessed with the dist.dna function of the APE R package (Paradis *et al.*, 2004) and plotted with the ggplot2 R package (Wickham, 2011).

is also congruent with recent studies on *L. arvensis* in which red- and blue-flowered plants were separated in different clades with nuclear microsatellite markers (Jiménez-López *et al.*, 2020b). In *L. monelli*, the strong support of our ITS phylogenetic results (80 BS, 0.850 PPS; Fig. 2) reinforced the hypothesis of taxon independency. Indeed, blue- and red-flowered lineages of *L. monelli* had been considered different subspecies or varieties (Ball, 1878; Jahandiez & Maire 1934).

In addition, colour lineages of *L. arvensis* or *L. monelli* were reconstructed as phylogenetically more closely related to other *Lysimachia* spp. than to each other. On the one hand, the blue-flowered plants of *L. arvensis* are sister to *L. talaverae* (clade I). This last taxon has already been recognized with the rank of species based only on morphological, ecological and karyological traits (Aymerich & Sáez, 2015), but not on molecular traits. Our study further validates the species rank status of *L. talaverae*. On the other hand, red-flowered individuals of *L. arvensis* are sister to red-flowered individuals of *L. monelli* (subclade A). Likewise, each of the colour lineages of *L. monelli* should be considered as different taxa. The blue

lineage of *L. monelli* was reconstructed as sister to *L. foemina* (subclade B), supporting the independence of *L. foemina* from *L. arvensis*, in accordance with Manns & Anderberg (2007b).

INCONGRUENCE BETWEEN NUCLEAR AND PLASTID PHYLOGENETIC RECONSTRUCTIONS

Colour lineages of both species appeared together with plastid DNA markers. Hybridization has been proposed as the cause of incongruences between phylogenetic trees based on plastid and nuclear DNA (Wendel & Doyle, 1998; Semerikova & Semerikov 2016). Hybridization involves past or present contact or hybrid zones (Petit, Bretagnolle & Felber, 1999), where lineages with divergent genomes have the potential to transfer alleles (Souissi *et al.*, 2017). However, as a result of this exchange it would be difficult to find a clear separation between lineages, contrasting with the strong separation between *Lysimachia* spp. using ITS (Fig. 2). Only one sample (LA_19B, blue *L. arvensis*) showed evidence of hybridization according to the recombination analyses.

Table 4. Summary statistics reported by the Species Delimitation plugin for ITS in each putative species: I, BI tree (clade support is PP); II, ML (clade support is %BS)

MOTU	Closest species	Clade support	Monophyletic?	Intra-/Inter	P ID(Strict)	Rosenberg's PAB	Rodrigo's P(RD)
I							
LA_R	LM_R	1	Yes	0.31	0.87 (0.80, 0.94)	7.3E-5*	0.0040*
LM_R	LA_R	1	Yes	0.21	0.73 (0.58, 0.87)	7.3E-5*	0.0033*
LF	LM_B	1	Yes	0.31	0.79 (0.69, 0.90)	1.21E-3*	0.0037*
LM_B	LF	0.999	Yes	0.10	0.73 (0.55, 0.90)	1.21E-3*	0.0011*
LA_B	LT	1	Yes	0.37	0.88 (0.83, 0.93)	1.0E-5*	0.0048*
LT	LA_B	1	Yes	0.17	0.75 (0.61, 0.89)	1.0E-5*	0.0021*
II							
LA_R	LM_R	95.55	Yes	1.09	0.41 (0.34, 0.48)	7.3E-5*	0.67
LM_R	LM_B	100	Yes	0.46	0.55 (0.41, 0.70)	7.3E-5*	0.69
LF	LM_B	100	Yes	0.91	0.41 (0.30, 0.66)	1.21E-3*	0.88
LM_B	LF	100	Yes	0.47	0.48 (0.30, 0.66)	1.21E-3*	0.14
LA_B	LT	100	Yes	1.10	0.47 (0.42, 0.53)	1.0E-5*	0.83
LT	LA_B	97.77	Yes	0.48	0.54 (0.40, 0.69)	1.0E-5*	0.37

Intra-/Inter, ratio of intraspecific genetic differentiation (among members of a putative species) to interspecific genetic differentiation (between the members of a putative species and the members of the closest putative species); P ID(Strict), mean (95% confidence interval) probability of correctly identifying an unknown member of a given clade using the criterion that it must fall within, but not sister to, the species clade in a tree; Rosenberg's P_{AB}, probability of reciprocal monophyly under a random coalescent model; Rodrigo's P(RD), probability that a clade has the observed degree of distinctiveness due to random coalescent processes.
*Significant values ($P < 0.05$, values remained significant after Bonferroni correction).

The position of this sample in the ITS tree (Supporting Information, Fig. S1) suggests possible hybridization between blue *L. arvensis* and *L. foemina*. These two taxa co-occur in some populations in Europe and their flowers are similar; thus, they possibly share pollinators. However, recombination analysis showed that this hybrid resulted from the crossing between red-flowered *L. arvensis* and *L. foemina*. Regardless, that hybridization originated from an individual with blue petals similar to the blue-flowered plants of *L. arvensis* (as was initially considered in the sampling). This hybrid (*L. arvensis* × *L. foemina*) has already been described as *A.* ×*doerfleri* Ronniger (Dörfler, 1903) [≡*Lysimachia* × *doerfleri* (Ronninger) Stace]. However, hybrid stabilization in natural populations seems difficult, as experimental crosses carried out by other authors frequently resulted in sterile F_1 progeny (Marsden-Jones, 1935; Kollmann & Feinbrun, 1968; Šveřepová, 1972).

The incongruent pattern observed between reconstructed phylogenetic trees based on nuclear and plastid DNA can be also explained by coalescent theory (Nordborg, 2001; Wakeley, 2009) because two or more alleles can coexist in the same ancestral population (Degnan & Rosenberg, 2009). Thus, the common ancestor of one group could have had the two plastid DNA haplotypes, one of which is currently present in red-flowered individuals of *L. arvensis* and *L. talaverae*, and the other in *L. monelli* and *L. foemina*, and both

haplotypes are present in blue-flowered individuals of *L. arvensis*. Later, segregation of colour lineages of *L. arvensis* and *L. monelli* probably occurred. That segregation could have been promoted by geographical separation, assortative mating mediated by pollinators or differential tolerance to abiotic factors, as has been described in other species (Kirkpatrick, 2000; Strauss & Whittal, 2006; Hopkins & Rausher, 2012; Wang *et al.*, 2013). In *L. monelli*, geographical separation could be contributing to lineage separation. However, in *L. arvensis* genetic flow is potentially possible between lineages in mixed populations although the reproductive isolation between them is high (F. J. Jiménez-López *et al.*, unpublished data); in fact, the results of nuclear phylogenetic reconstruction point towards a clear isolation of both colour lineages.

THE ROLE OF FLOWER COLOUR IN SPECIATION IN MEDITERRANEAN *LYSIMACHIA*

Flower colour constitutes a pivotal evolutionary force to speciation in several groups of plants (Carlson & Holsinger, 2015; Ellis & Field, 2016; Takahashi, Takakura & Kawata, 2016; Narbona *et al.*, 2018), and it has been proposed as a 'magic trait', that is a trait 'encoded by genes subjected to divergent selection that affect pleiotropically reproductive isolation' (Servedio *et al.*, 2011). However, according to ancestral state reconstruction, flower colour does not seem the
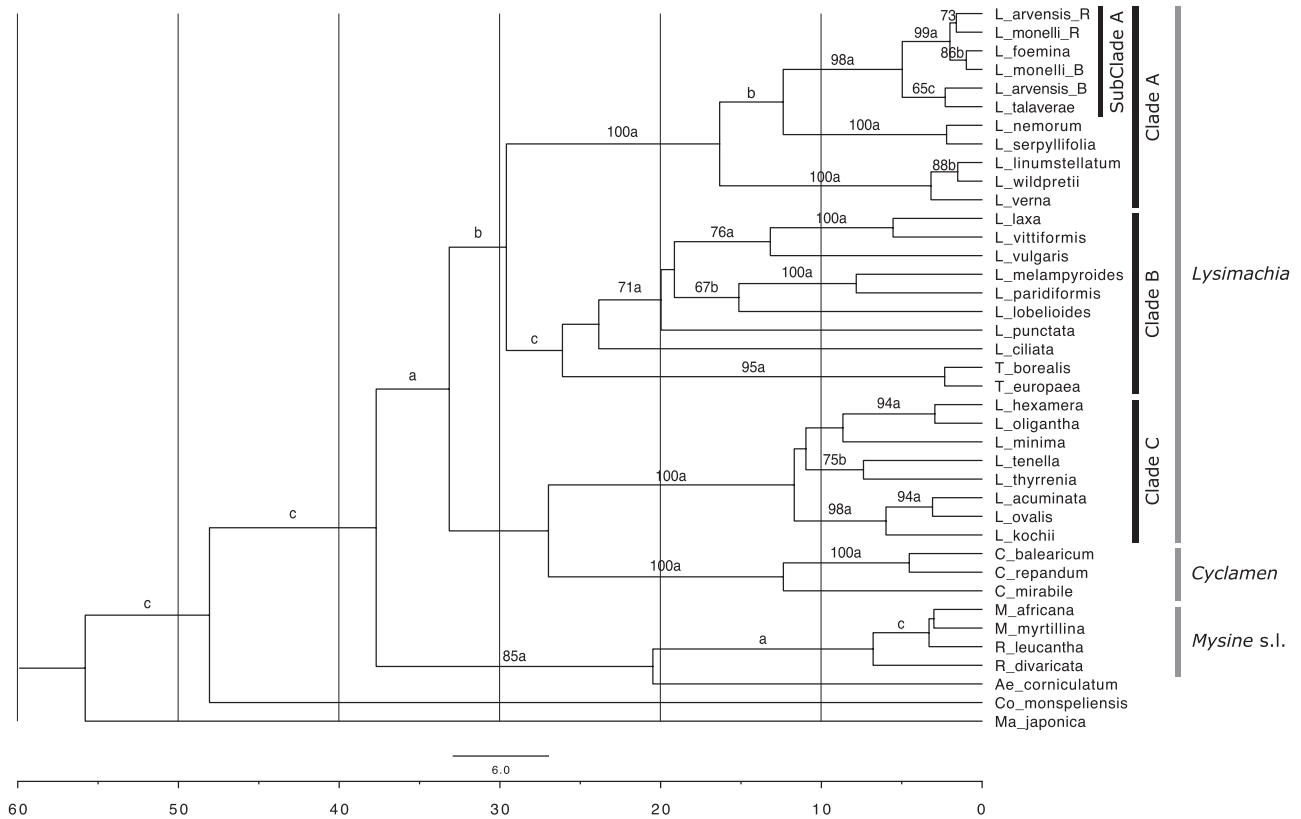
Figure 5. Phylogenetic reconstruction for tribe Lysimachieae. Maximum clade credibility (MCC) tree reconstructed with BEAST based on internal transcribed spacer (ITS) data for *Lysimachia* spp. and related genera of Lysimachieae. Abbreviations for other genera: *Aegicera* (Ae), *Coris* (Co), *Cyclamen* (C), *Maesa* (Ma), *Myrsine* (M) and *Rapanea* (R); see Supporting Information, Table S3. The root was calibrated following Yan *et al.* (2018), a *Maesa* sp. fossil (Huzioka & Takahasi, 1970) and a Yule speciation tree prior. Bootstrap support > 65% of the ML estimate (RAxML) and posterior probabilities of the Bayesian approach (BEAST; PPS value coded as a = 0.995–1.000, b = 0.950–0.994 or c = 0.850–0.950) are given above branches.

trait promoting divergence between lineages of *L. arvensis*, although it does in *L. monelli* with posterior polyploidization events (see below). Ancestral state reconstruction of this trait invoked a blue-flowered common ancestor for this Mediterranean *Lysimachia*, and the transition to red-flowered plants probably occurred only once for the red-flowered common ancestor of red *L. arvensis* and red *L. monelli*. This kind of transition from blue to red flowers is quite frequent due to inactivation of a branch of the anthocyanin pathway (Rausher, 2008), and it has been found in *L. arvensis* lineages (Sánchez-Cabrera *et al.*, 2021). In other plant groups, red-flowered species are usually derived from blue-flowered species (Kay *et al.*, 2005; Wilson *et al.*, 2007; Rausher, 2008; Wessinger & Rausher, 2012). In our study, the blue ancestor probably gave rise to two lineages, one entirely blue (which includes the blue lineage of *L. arvensis*) and another that subsequently separated into blue- and a red-flowered subclades (the latter including the red

lineage of *L. arvensis* and *L. monelli*). According to the results of diversification time estimation, this second diversification event occurred *c*. 2.1 Mya, slightly after the onset of the Mediterranean climate (3.4–2.8 Mya). As a consequence of this palaeoclimatic event, a wealth of diversity has been reported in native Mediterranean plant species (e.g. Postigo *et al.*, 2009; Jiménez-Moreno, Fauquette & Suc., 2010). *Lysimachia monelli* may have been influenced by warm and cold episodes in the Pleistocene affecting its current geographical distribution and genetic structure, as reported in other Mediterranean groups of plants (Vargas, 2003). However, this aspect requires future research, because no evidence of distinct ecological niches between *L. monelli* colour lineages has been published so far. On the other hand, the estimated diversification time (5.1 Mya) and the location of each *L. arvensis* colour lineage in the phylogenetic reconstruction suggests independent origins for colour lineages of this species, possibly influenced by arid-adapted

lineage diversification during the Messinian Salinity Crisis (Rodríguez-Sánchez *et al.*, 2008). In fact, Arista *et al.* (2013) demonstrated the adaptation to drought and high sunshine conditions of the blue *L. arvensis* lineage. Hence, these results indicate that flower colour cannot have been the trigger for the current speciation of *L. arvensis* colour lineages, and future analyses are required to clarify the role of flower colour in the speciation of *L. monelli*.

THE ROLE OF PLOIDY IN SPECIATION IN *LYSIMACHIA*

Although the role of polyploidy in the evolution of *Lysimachia* taxa was not the aim of this study, the relationship between the studied species and their ploidy clearly suggests an important role in speciation. Although patterns of chromosome transition have not been essential in species diversification in the Mediterranean basin (Escudero *et al.*, 2018), this clade of *Lysimachia* could be an exception, and a clear example of the role of polyploidy in rapid speciation. According to the phylogenetic tree constructed with ITS, diploid and tetraploid taxa appear together in each clade: the blue lineage of *L. monelli* ($2x$) with *L. foemina* ($4x$), *L. talaverae* ($2x$) with the blue lineage of *L. arvensis* ($4x$), and the red lineage of *L. monelli* ($2x$) with the red lineage of *L. arvensis* ($4x$). Polyploid speciation implies complete duplication of the genome after hybridization (allopolyploidy) or duplication of complete genomes (autopolyploidy). The configuration observed in the phylogenetic reconstruction (Fig. 2) suggests that both colour lineages of *L. arvensis*, which are tetraploid, originated via autopolyploidy. In phylogenetic studies it is important to consider that multiple copies of the ITS region are often homogenized by concerted evolution (Volkov *et al.*, 1999). In allopolyploids ITS variants tend to be on different chromosomes, and their homogenization should proceed less efficiently than in autotetraploids in which differences between alleles are in the same chromosomes. Thus, a greater persistence of different ITS variants and a higher number of polymorphic sites are expected in allopolyploids (O'Kane, Schaal & Al-Shehbaz., 1996). Although the sequence data obtained here do not allow specific inference of the origin of the tetraploid species, lack of polymorphisms within taxa and the low genetic differences among tetraploids and the closest diploid taxa (Table 2) point to a recent autopolyploid origin (e.g. Lihová *et al.* 2004). We suggest that red *L. arvensis* could derive from red *L. monelli* (diploid), and blue *L. arvensis* could derive from *L. talaverae* (diploid with blue flowers). Moreover, *L. foemina* (tetraploid with blue flowers) could derive from blue *L. monelli* (diploid). At least for *L. arvensis*, both colour lineages have a karyotype with four equal copies of a set of chromosomes (Monein, Atta & Shehata., 2003)

and the chromatograms of ITS sequences were highly stable [Percentage of high quality (HQ%) > 80% in *L. arvensis*], supporting the autopolyploid origin of these taxa. This would indicate the presence of multiple polyploidization events in the clade studied, as found in other genera (e.g. Rieseberg *et al.*, 2003; Wang *et al.*, 2006; Wood *et al.*, 2009; Soltis *et al.*, 2015; Padilla-García *et al.*, 2018). Divergence-time estimation between the diploid and tetraploid taxa, *c*. 1 Mya (Fig. 5), and the support of the phylogenetic reconstruction (Fig. 2) point to recent tetraploidization events, and the stability in the genomic sequences studied also suggests an autopolyploid origin, in accordance with current evolutionary theories on polyploids (Otto & Whitton, 2000; Soltis, Visger & Soltis, 2014; Soltis *et al.*, 2015). However, the possible role of polyploidy in the evolution of the studied *Lysimachia* would need a more directed study.

CONCLUSIONS

The colour morphs of either *L. arvensis* or *L. monelli* constitute independent species. Although our results indicated that flower colour has not triggered recent speciation events in this group, it can have an important role as a reinforcement mechanism that prevents the formation of maladapted hybrids (Hopkins, 2013). This could be the situation at least in *L. arvensis*, in which pollinators prefer the blue lineage and scarcely made transitions between flowers of different colours (Ortiz *et al.*, 2015; Jiménez-López *et al.*, 2020a). The low frequency of hybrids in mixed-colour populations (Jiménez-López *et al.*, 2020c) and the lack of hybrid samples found in the present study support the importance of colour as a reinforcement mechanism.

TAXONOMIC IMPLICATIONS

Our results have taxonomic implications for the colour lineages of *L. arvensis* and *L. monelli* as each lineage should be defined as different taxa supported by morphological, phylogenetic and geographical data. Thus, we propose the following names or combinations:

- *Lysimachia arvensis* (L.) U.Manns & Anderb. in Willdenowia, 39(1):51. (2009) ≡ *Anagallis arvensis* L., Sp. Pl.: 148. 1753, [basion.] ≡ *Anagallis arvensis* var. *phoenicea* Gouan, Fl. Mons.: 24 (1764), nom. illeg. ≡ *Anagallis phoenicea* (Gouan) Scop., Fl. Carn. ed. 2, 1: 139 (1777), nom. illeg. ≡ *Anagallis arvensis* subsp. *phoenicea* (Gouan) Wallmann in Ber. Bayer. Bot Ges. 9: 44 (1904), nom. inv.

Ind. Loc.: 'Habitat in Europae arvis'.

Lectotype designated by Dyer (1963): 14: Herb. Linn. 208.1 (LINN)

Red-flowered plants of *Lysimachia arvensis* should maintain this name because Linnaeus in 1753 described the species from red-flowered plants.

- *Lysimachia loeflingii* **F.J.Jiménez-López & M.Talavera, nom. nov.** ≡ *Anagallis latifolia* L., Sp. Pl. 1: 149 (1753) [syn. subst.] ≡ *A. arvensis* subsp. *latifolia* (L.) Arcang., Comp. Fl. Ital., ed.2: 456 (1894) - *Anagallis arvensis* L. subsp. *arvensis* var. *caerulea sensu* Kollmann & Feinbrun in Notes Royal Bot. Gard. Edinburgh 27: 176 (1968), non *A. arvensis* L. var. *caerulea* (L.) Gouan, Fl. Monsp.: 30 (1765)

Ind. loc.: 'Habitat in Hispania Loef.'

Lectotype designated here: Herb. Linn. 208.3, 'H.U.3. latifolia. ex Hispanica foly amplexicauly' [m. Linnaeus]

Blue plants of *L. arvensis* should be called with the specific epithet *latifolia* as it was the first name employed by Linnaeus in 1753 for plants with blue flowers. However, the epithet *latifolia* already exists in *Lysimachia* for a different taxon [*Lysimachia latifolia* (Hook.) Cholewa in Phytoneuron 28: 1–2 (2014) = *Trientalis latifolia* Hook., Fl. Bor. Amer. 2(9): 121 (1839), a plant described from Washington]. Therefore, we have selected the name *L. loeflingii* because Linnaeus in 1753 described blue-flowered plants from materials collected by Loefling in Spain.

Anagallis latifolia L. was described by Linnaeus in the 1st edition of *Species Plantarum* (1753: 149) indicating: '3. Anagallis foliis cordatis amplexicaulibus, caulibus compressis latifolia/ Anagallis hispanica, latifolia, maximum flore. Tournef. Inst. 142/ Cruciata Montana minor, flore caeruleo. Barr. Ic. 584/ Habitat in Hispania Loefl.'

Linnaeus described that plant indicating the colour of the flowers, '*Corolla caerulea, fondo purpurascens*' and that of the stamens, '*Filamenta purpurea. Antheris oblongis, flavis*'.

The reference made by Linnaeus to Tournefort (1719: 142) corresponds, according to Sampaio (1900: 57), to a plant collected by Tournefort in 'Ultra San Joan de Foz ad ostium durii' on his travel through Portugal in 1689, as it appears in a manuscript that Tournefort left in the Museu Botanico da Universidade (Coimbra). This phrasal name of Tournefort was used by Sampaio (1900: 58) as a synonym of *Anagallis hispanica* Sampaio, which we consider here synonymous of *Anagallis monelli* L. (see below this species). Furthermore, the icon 584, in Lam. 157, of Barrelier (1714: 17) represented faithfully the upper part of a branch with large flowers and with all the leaves arranged in verticils of four at each node. This plant can also be identified as *Anagallis monelli* L. So, none of the synonyms given by Linnaeus in *A. latifolia* could be used to choose the type of *L. loeflingii*. Both

Tournefort's plant and Barrelier's icon have different characters from those described by Linnaeus in *A. latifolia*. Therefore, the type would have to be chosen from the herbarium material sent by Loefling to Linnaeus from Spain, as indicated by Linnaeus for the type locality.

- *Lysimachia talaverae* L.Sáez & Aymerich in Orsis 29: 48 (2015) ≡ *Anagallis parviflora* Hoffmanns. & Link, Fl. Portug. 1 (11): 325, 326. Tab. 64 (1813–1820) [syn. subst.] ≡ *Anagallis arvensis* subsp. *parviflora* (Hoffmanns. & Link) Arcangeli, Comp. Fl. Ital. ed.2: 456 (1894) = *Anagallis latifolia* 'raza' *parviflora* (Hoffmanns. & Link) Merino in Broteria, sér. Bot. 14: 162 (1916), nom. illeg.

Ind. loc.: 'Dans les lieux sablonneux aux environs de Comporta'.

Plants with small blue flowers that live in a wetland environment have been included sometimes in *Anagallis arvensis*, and thus a typification proposal is made. Lectotype designated here (iconotype): *Anagallis parviflora* Tab. 64 in Hoffmannsegg & Link, Fl. Portug. 1 (13): 326 (1813–1820).

Epitype: Huelva. Hinojos, Las Porqueras. Lagoon edge. 37°17′37″N–6°25′15″W. 108 m. 5/5/2014. Leg. F.J. Jiménez & S. Talavera. SEV286467. A sheet of this sample has been included, among others, in this study to establish the phylogenetic reconstruction.

- *Lysimachia monelli* (L.) U. Manns & Anderb. in Willdenowia, 39(1): 52 (2009) ≡ *Anagallis monelli* L., Sp. Pl. 1: 148 (1753), [basionym].

Ind. Loc.: not indicated by Linnaeus in 1753; 'Habitat in Verona' in Linnaeus, Sp. Pl. ed. 2, 1: 212. 1762. As indicated by Pau (1915) the type locality indication was clearly exposed by Linnaeus when he described the species when indicating his previous synonym, in *Hortus Cliffortianus*, 52. 1738: 'Crecit forte Gadibus und seminis accepit Joh. Monellus Tornacensis, atque eaden cum Clussius comunicavit anno 1602', and in *Hortus Upsaliensis*, 38. 1748: 'Habitario incerta. Johannes Monellus 1662 Gadibus semina Clussius misit. Hospitatur in Terpidario, perennes'.

Lectotype designated by Manns & Anderberg in Willdenowia 39 (1): 52 (2009): Hort. Cliff. 52.2, Anagallis 2 (BM000557969).

Lysimachia monelli should be referred exclusively to the blue lineage because it was used by Linnaeus in 1753 to describe this species for the first time. The lectotype (!photograph) consists of two flowering stems of *c.* 30 cm, one undivided and the other branched almost from the base, with numerous flowers but only those of the apex in anthesis, the others in postanthesis; internodes 2–5 cm, longer than the leaves; opposite inferior leaves, of 20–25 × 5 mm, elliptical, attenuate

at the base, acute in the apex, superior in whorls of three leaves of 15–20 × 3–5 mm, elliptical, each one with a long pedicelled flower; pedicels of 25–35 mm, generally larger than the leaves. These branches come from the garden of George Clifford III (Hartekamp Garden, Holland).

= *Anagallis linifolia* L. Sp. Pl. ed. 2, 1: 212 (1762)

≡ *Anagallis monelli* subsp. *linifolia* Maire in Jahandiez & Maire, Cat. Pl. Maroc.: 562 (1934)

Ind. Loc.: 'Habitat in Lusitania, Hispania. Claud Alstroemer'

Lectotype designated here: 'linifolia [m. Linnaeus] A [Alstroemer]': Herb. Linn. 208.4 (LINN-ML)

The lectotype is formed by a single, apparently, annual plant 10 cm high, erect, with three short branches with fruits in the upper half, and other branches emerging near to the axonomorph root; stem with very short internodes, surpassed by the leaves; leaves of 6–10 × 0.1–0.2 mm, narrowly linear, truncated at the base, obtuse; recurved and rigid pedicels in well-developed fruits; fruits shorter than the calyx. The characters of this plant coincide with those indicated by Linnaeus when he described the species, so there is no doubt that this plant is the same as Linnaeus saw. The indication 'Lusitania' could have been made by Linnaeus from a plant from Portugal described by Tournefort and cited as a synonym.

- *Lysimachia collina* (Schousb.) FJ.Jiménez-López, comb. nov. ≡ *Anagallis collina* Schousb., Iagttag. Vextrig. Marokko.: 78. (1800), basion. ≡ *Anagallis monelli* subsp. *collina* (Schousb.) H.Lindb. in Acta Soc. Sci. Fenn., ser. B, Opera Biol. 1(2): 115. (1932). ≡ *Anagallis monelli* var. *collina* (Schousb.) Pau in Mem. Real. Soc. Esp. Hist. Nat. 12 (5): 360 (1924) ≡ *Anagallis linifolia* var. *collina* (Schousb.) Ball in J. Linn. Soc. 16: 562 (1878). ≡ *Anagallis linifolia* f. *rubriflora* Batt. in Battandier & Trabut, Fl. Algérie, Dicot.: 723 (1890), [syn. subst.].

Ind. loc.: 'Frequens ocurrit in collibus aridis provinciae Haha'

Red plants of *L. monelli* should be referred to *L. collina* because plants with this colour were described by Schousboe in 1800 as *Anagallis collina*. Due to *Anagallis* now being included in *Lysimachia*, we make a new combination.

Lectotype designated here: Mogador [Haha] Schousboe [m. Schousboe]: C 10001180.

The type material consists of a single woody stem of 15 cm length, without leaves in the lower half,

---

DETERMINATION KEY

1. Perennial plants, rarely annual herbs with a single stem; stem nodes with (two) three or four (five) verticillated leaves; fertile nodes with a single flower in the axil of each leaf; flowers with the corolla (14) 16–25 mm in diameter, styles 3–4 mm in length **2**
- Annual plants; nodes generally with opposite leaves, rarely with three verticillated leaves; fertile nodes with two flowers, one in each leaf axil, rarely with a single flower; flowers with corolla 3–12 (14) mm in diameter; styles 1.0–2.5 mm in length **3**
2. Flowers with orange or red corolla.. *Lysimachia collina*
- Flowers with blue corolla .... *Lysimachia monelli*
3. Plants generally compact; internodes generally shorter than the leaves; leaves, at least the upper ones, erect-patent, lanceolate or elliptic-lanceolate, acute; fruit pedicels generally shorter than internodes; flowers with blue corolla, with elliptical lobes, strongly serrated in the upper half of the margin, covered with hairs with (three) four (five) cells, the terminal elliptical or sub-cylindrical, about the size and shape of the adjacent cell, sometimes glabrous .... *Lysimachia foemina*
- Plants generally graceful; internodes often longer than leaves; leaves patent, ovate or ovate-lanceolate, obtuse or subacute; fruit pedicels generally larger than internodes; flowers with blue or orange-red corolla, with lobes broadly ovate, denticulate, with the margin densely covered with hairs with three cells, the terminal globose, larger than the underlying cell **4**
4. Flowers blue **5**
- Flowers orange or red .... *Lysimachia arvensis*
5. Small plants, generally < 10 cm in length; root neck generally covered by secondary roots; ovate leaves; flowers with blue or pale blue corolla, often surpassed by calyx; styles 1.0–1.5 mm in length; .... *Lysimachia talaverae*
- Generally large plants, up to 60 cm in length; bare root neck without secondary roots; ovate-lanceolate leaves, at least in the upper half of the stem; blue corolla, usually longer than the calyx; styles 2.0–2.5 mm in length .... *Lysimachia loeflingii*

branched in the upper half; each branch short, with some oval–lanceolate leaves, acute, shorter than the pedicels and the majority of the flowers in anthesis; isolectotype C 10001181.

ACKNOWLEDGEMENTS

REFERENCES

Anderberg AA, **Manns U**, **Källersjö M. 2007.** Phylogeny and floral evolution of the Lysimachieae (Ericales, Myrsinaceae). Evidence from *ndhF* sequence data. *Willdenowia* **37:** 407–421.

Arcangeli G. 1894. *Compendio della Flora Italiana*, **Vol. 2**. Turin: E. Loescher, 456.

Arista M, **Talavera M**, **Berjano R**, **Ortiz PL. 2013.** Abiotic factors may explain the geographical distribution of flower colour morphs and the maintenance of colour polymorphism in the scarlet pimpernel. *Journal of Ecology* **101:** 1613–1622.

Armbruster WS. 1997. Exaptations link the evolution of plant–herbivore and plant–pollinator interactions: a phylogenetic inquiry. *Ecology* **78:** 1661–1674.

Armbruster WS. 2002. Can indirect selection and genetic context contribute to trait diversification? A transition-probability study of blossom-colour evolution in two genera. *Journal of Evolutionary Biology* **15:** 468–486.

Aymerich P, **Sáez Ll. 2015.** Comentaris i precisions previs a la Checklist de la flora de Catalunya (Nord-Est de la península Ibèrica). *Orsis* **29:** 23–90.

Ball J. 1878. Introductory observations to the *Spicilegium Florae Maroccanae*. *Journal of the Linnean Society* **16:** 377–772.

Baum DA, **Shaw KL**, **Hoch PC**, **Stephenson AG. 1995.** Genealogical perspectives on the species problem, Experimental and molecular approaches to plant biosystematics. *St. Louis Missouri Botanical Garden,* 289–303.

Barrelier J. 1714. *Plantae per Galliam, Hispaniam et Italiam*. Ed. Antoine de Joussieu. Parisii.

Bouckaert R, **Vaughan TG**, **Barido-Sottani J**, **Duchêne S**, **Fourment M**, **Gavryushkina A**, **Heled J**, **Jones G**, **Kühnert D**, **De Maio N**, **Matschiner M**, **Mendes FK**, **Müller NF**, **Ogilvie HA**, **du Plessis L**, **Popinga A**, **Rambaut A**, **Rasmussen D**, **Siveroni I**, **Suchard MA**, **Wu CH**, **Xie D**, **Zhang C**, **Stadler T**, **Drummond AJ. 2019.** BEAST 2.5: an advanced software platform for Bayesian evolutionary analysis. *PLoS Computational Biology* **15:** e1006650.

Carlson JE, **Holsinger KE. 2015.** Extrapolating from local ecological processes to genus-wide patterns in colour polymorphism in South African Protea. *Proceedings of the Royal Society B: Biological Sciences* **282:** 20150583.

Chase MW, **Hills HG. 1991.** Silica gel: an ideal material for field preservation of leaf samples for DNA studies. *Taxon* **40:** 215–220.

Darriba D, **Taboada GL**, **Doallo R**, **Posada D. 2012.** jModelTest 2: more models, new heuristics and parallel computing. *Nature Methods* **9:** 772.

Degnan JH, **Rosenberg NA. 2009.** Gene tree discordance, phylogenetic inference and the multispecies coalescent. *Trends in Ecology & Evolution* **24:** 332–340.

Dörfler I. 1903. *Herbarium Normale*, **Vol. 45**. Vienna: O. Hensel, 143.

Drummond AJ, **Ho SY**, **Phillips MJ**, **Rambaut A. 2006.** Relaxed phylogenetics and dating with confidence. *PLoS Biology* **4:** e88.

Duminil J, **Di Michele M. 2009.** Plant species delimitation: a comparison of morphological and molecular markers. *Plant Biosystems* **143:** 528–542.

Dyer RA. 1963. *Primulaceae*. In: Dyer RA, Codd IE, Rycroft HB. eds. *Flora of southern Africa*. Pretoria: Government Printer, 9–14.

Dyer AG, **Boyd-Gerny S**, **Shrestha M**, **Lunau K**, **Garcia JE**, **Koethe S**, **Wong BB. 2016.** Innate colour preferences of the Australian native stingless bee *Tetragonula carbonari*a Sm. *Journal of Comparative Physiology. A, Neuroethology, Sensory, Neural, and Behavioral Physiology* **202:** 603–613.

Ellis TJ, **Field DL. 2016.** Repeated gains in yellow and anthocyanin pigmentation in flower colour transitions in the Antirrhineae. *Annals of Botany* **117:** 1133–1140.

Escudero M, **Balao F**, **Martín-Bravo S**, **Valente L**, **Valcárcel V. 2018.** Is the diversification of Mediterranean Basin plant lineages coupled to karyotypic changes? *Plant Biology (Stuttgart, Germany)* **20 (Suppl. 1):** 166–175.

Farris JS, **Källersjö M**, **Kluge AG**, **Bult C. 1994.** Testing significance of congruence. *Cladistics* **10:** 315–320.

Ferguson LF. 1972. *Anagallis* L. In: Tutin TG, Heywood VH, Burges NA, Moore DM, Valentine DH, Walters SM,

Webb DA. eds. *Flora Europea 3, Diapensiaceae-Myoporaceae*. Cambridge: Cambridge University Press, 28–29.

Fiz-Palacios O, **Valcárcel V. 2013.** From Messinian crisis to Mediterranean climate: a temporal gap of diversification recovered from multiple plant phylogenies. *Perspectives in Plant Ecology, Evolution and Systematics* **15:** 130–137.

Frey FM. 2004. Opposing natural selection from herbivores and pathogens may maintain floral-color variation in *Claytonia virginica* (Portulacaceae). *Evolution; International Journal of Organic Evolution* **58:** 2426–2437.

Freyre R, **Griesbach RJ. 2004.** Inheritance of flower color in *Anagallis monelli* L. *HortScience* **39:** 1220–1223.

Friis EM. 1985. Angiosperm fruits and seeds from the Middle Miocene of Jutland (Denmark). *Det Kongelige Danske Videnskaberne Selskab* **24:** 1–165.

García Pérez L, **Talavera S**, **Ortiz PL**, **Arista M. 1997.** Números cromosomáticos de plantas occidentales 734-737. *Anales del Jardín Botánico de Madrid* **55:** 344–345.

Gibbs PE, **Talavera S. 2001.** Breeding system studies in three species of *Anagallis* (Primulaceae): self-incompatibility and reduced female fertility in *A. monelli* L. *Annals of Botany* **88:** 139–144.

de Halácsy E. 1904. *Conspectus Florae Graecae*, **Vol. 3**. Leipzig: Engelmann.

Hamilton MB. 1999. Four primer pairs for the amplification of chloroplast intergenic regions with intraspecific variation. *Molecular Ecology* **8:** 521–523.

Hanusch M, **Ortiz EM**, **Patiño J**, **Schaefer H. 2020.** Biogeography and integrative taxonomy of *Epipterygium* (Mniaceae, Bryophyta). *Taxon* **69:** 1150–1171.

Heled J, **Drummond AJ. 2012.** Calibrated tree priors for relaxed phylogenetics and divergence time estimation. *Systematic Biology* **61:** 138–149.

Ho SY, **Phillips MJ. 2009.** Accounting for calibration uncertainty in phylogenetic estimation of evolutionary divergence times. *Systematic Biology* **58:** 367–380.

Hoffmannsegg JCG, **Link JHF. 1813-1820.** *Flore Portugaise, 1 (11).* Berlin: Charles Fréderic Amelang, 325 Tab. 64.

Hopkins R. 2013. Reinforcement in plants. *The New Phytologist* **197:** 1095–1103.

Hopkins R, **Rausher MD. 2012.** Pollinator-mediated selection on flower color allele drives reinforcement. *Science (New York, N.Y.)* **335:** 1090–1092.

Huelsenbeck JP, **Nielsen R**, **Bollback JP. 2003.** Stochastic mapping of morphological characters. *Systematic Biology* **52:** 131–158.

Huxley JS. 1955. Morphism and evolution. *Heredity* **9:** 1–51.

Huzioka K, **Takahasi E. 1970.** The Eocene flora of the Ube coal-field, southwest Honshu, Japan. *Journal of the Mining College, Akita University, Series A: Mining Geology* **4:** 1–88.

Ishikura N. 1981. Flavonoids in the petal cells of *Anagallis arvensis* f. *coerulea* containing a blue crystalline anthocyanin. *Zeitschrift für Pflanzenphysiologie* **103:** 469–473.

Jahandiez E, **Maire R. 1934.** *Catalogue des plantes du Maroc*, **Vol 3**. Algiers: Imprimerie Minerva, 563.

Jiménez-López FJ, **Matas L**, **Arista M**, **Ortiz PL. 2020a.** Flower colour segregation and flower discrimination under the bee vision model in the polymorphic *Lysimachia arvensis*. *Plant Biosystems* **154:** 535–543.

Jiménez-López FJ, **Ortiz MA**, **Berjano R**, **Talavera S**, **Terrab A. 2016.** High population genetic substructure in *Hypochaeris leontodontoides* (Asteraceae), an endemic rupicolous species of the Atlas Mountains in NW Africa. *Alpine Botany* **126:** 73–85.

Jiménez-López FJ, **Ortiz PL**, **Talavera M**, **Arista M. 2020b.** Reproductive assurance maintains red-flowered plants of *Lysimachia arvensis* in Mediterranean populations despite inbreeding depression. *Frontiers in Plant Science* **11:** 563110.

Jiménez-López FJ, **Ortiz PL**, **Talavera M**, **Pannell JR**, **Arista M. 2020c.** The role of lateral and vertical herkogamy in the divergence of the blue- and red-flowered lineages of *Lysimachia arvensis*. *Annals of Botany* **125:** 1127–1135.

Jiménez-Moreno G, **Fauquette S**, **Suc JP. 2010.** Miocene to Pliocene vegetation reconstruction and climate estimates in the Iberian Peninsula from pollen data. *Review of Palaeobotany and Palynology* **162:** 410–415.

Kapli P, **Lutteropp S**, **Zhang J**, **Kobert K**, **Pavlidis P**, **Stamatakis A**, **Flouri T. 2017.** Multi-rate Poisson tree processes for single-locus species delimitation under maximum likelihood and Markov chain Monte Carlo. *Bioinformatics (Oxford, England)* **33:** 1630–1638.

Kay KM, **Reeves PA**, **Olmstead RG**, **Schemske DW. 2005.** Rapid speciation and the evolution of hummingbird pollination in neotropical *Costus* subgenus *Costus* (Costaceae): evidence from nrDNA ITS and ETS sequences. *American Journal of Botany* **92:** 1899–1910.

Kimura M. 1980. A simple method for estimating evolutionary rates of base substitutions through comparative studies of nucleotide sequences. *Journal of Molecular Evolution* **16:** 111–120.

Kirkpatrick M. 2000. Reinforcement and divergence under assortative mating. *Proceedings of the Royal Society B: Biological Sciences* **267:** 1649–1655.

Kollmann F, **Feinbrun N. 1968.** A cyto-taxonomic study in Palestinian *Anagallis arvensis* L. *Notes of the Royal Botanic Garden Edinburgh* **27:** 173–186.

Kress A. 1969. Cytotaxonomic studies on Primulaceae. *Phyton* **13:** 211–225.

Krijgsman W, **Stoica M**, **Vasiliev I**, **Popov VV. 2010.** Rise and fall of the Paratethys Sea during the Messinian Salinity Crisis. *Earth and Planetary Science Letters* **290:** 183–191.

Kumar S, **Stecher G**, **Li M**, **Knyaz C**, **Tamura K. 2018.** MEGA X: molecular evolutionary genetics analysis across computing platforms. *Molecular Biology and Evolution* **35:** 1547–1549.

Levin DA, **Brack ET. 1995.** Natural selection against white petals in *Phlox*. *Evolution; International Journal of Organic Evolution* **49:** 1017–1022.

Lihová J, **Fuertes Aguilar J**, **Marhold K**, **Nieto Feliner G. 2004.** Origin of the disjunct tetraploid *Cardamine amporitana* (Brassicaceae) assessed with nuclear and chloroplast DNA sequence data. *American Journal of Botany* **91:** 1231–1242.

Linnaeus C. 1753. *Species Plantarum*, **Vol. 1**. Stockholm: Impensis Laurentii Salvii, Holmiae, 148–149.

Lunau K, **Maier EJ. 1995.** Innate colour preferences of flower visitors. *Journal of Comparative Physiology A* **177:** 1–19.

Magallón S, **Hilu KW**, **Quandt D. 2013.** Land plant evolutionary timeline: gene effects are secondary to fossil constraints in relaxed clock estimation of age and substitution rates. *American Journal of Botany* **100:** 556–573.

Manns U, **Anderberg AA. 2005.** Molecular phylogeny of *Anagallis* (Myrsinaceae) based on ITS, *trnL-F*, and *ndhF* sequence data. *International Journal of Plant Sciences* **166:** 1019–1028.

Manns U, **Anderberg AA. 2007a.** Character evolution in *Anagallis* (*Myrsinaceae*) inferred from morphological and molecular data. *Systematic Botany* **32:** 166–179.

Manns U, **Anderberg AA. 2007b.** Relationships of *Anagallis foemina* and *A. arvensis* (Myrsinaceae): new insights inferred from DNA sequence data. *Molecular Phylogenetics and Evolution* **45:** 971–980.

Manns U, **Anderberg AA. 2009.** New combinations and names in *Lysimachia* (*Myrsinaceae*) for species of *Anagallis*, *Pelletiera* and *Trientalis*. *Willdenowia* **39:** 49–54.

Marsden-Jones EM. 1935. The genetic of *Anagallis arvensis* Linn. and *Anagallis foemina* Mill. *Proceedings of the Linnean Society of London* **147:** 105–106.

Marsden-Jones EM, **Weiss FE. 1938.** The essential differences between *Anagallis arvensis* Linn. and *Anagallis foemina* Mill. *Proceedings of the Linnean Society of London* **150:** 146–155.

Martin DP, **Murrell B**, **Golden M**, **Khoosal A**, **Muhire B. 2015.** RDP4: detection and analysis of recombination patterns in virus genomes. *Virus Evolution* **1:** vev003.

Martins L, **Oberprieler C**, **Hellwig FH. 2003.** A phylogenetic analysis of *Primulaceae s.l.* based on internal transcribed spacer (ITS) DNA sequence data. *Plant Systematics and Evolution* **237:** 75–85.

Masters BC, **Fan V**, **Ross HA. 2011.** Species delimitation – a Geneious plugin for the exploration of species boundaries. *Molecular Ecology Resources* **11:** 154–157.

Miller MA, **Pfeiffer W**, **Schwartz T. 2010**. Creating the CIPRES Science Gateway for inference of large phylogenetic trees. In: *Proceedings of the Gateway Computing Environments Workshop (GCE)*, New Orleans, ACM Journals, 1–8.

Monein A, **Atta II**, **Shehata AA. 2003.** On the delimitation of *Anagallis arvensis* L. (Primulaceae) 1. Evidence based on micromorphological characters, palynological features and karyological studies. *Pakistan Journal of Biological Sciences* **6:** 29–35.

Narbona E, **Wang H**, **Ortiz PL**, **Arista M**, **Imbert E. 2018.** Flower colour polymorphism in the Mediterranean Basin: occurrence, maintenance and implications for speciation. *Plant Biology* **20:** 8–20.

Nordborg M. 2001. Coalescent theory. In: Balding DJ, Bishop M, Cannings C, eds. *Handbook of statistical genetics*. Chichester: John Wiley & Sons, 179–212.

O'Kane SL, **Schaal BA**, **Al-Shehbaz IA. 1996.** The origins of *Arabidopsis suecica* (Brassicaceae) as indicated by nuclear rDNA sequences. *Systematic Botany* **21:** 559–566.

Oh IC, **Anderberg AL**, **Schönenberger J**, **Anderberg AA. 2008.** Comparative seed morphology and character evolution in the genus *Lysimachia* (Myrsinaceae) and related taxa. *Plant Systematics and Evolution* **271:** 177–197.

Ortiz PL, **Berjano R**, **Talavera M**, **Rodríguez-Zayas L**, **Arista M. 2015.** Flower colour polymorphism in *Lysimachia arvensis*: how is the red morph maintained in Mediterranean environments? *Perspectives in Plant Ecology, Evolution and Systematics* **17:** 142–150.

Otto SP, **Whitton J. 2000.** Polyploid incidence and evolution. *Annual Review of Genetics* **34:** 401–437.

Padilla-García N, **Rojas-Andrés BM**, **López-González N**, **Castro M**, **Castro S**, **Loureiro J**, **Albache DC**, **Machon N**, **Martínez-Ortega MM. 2018.** The challenge of species delimitation in the diploid–polyploid complex *Veronica* subsection *Pentasepalae*. *Molecular Phylogenetics and Evolution* **119:** 196–209.

Paradis E, **Claude J**, **Strimmer K. 2004.** APE: analyses of phylogenetics and evolution in R language. *Bioinformatics (Oxford, England)* **20:** 289–290.

Pastor J. 1992. *Atlas cromosómico de la flora vascular de Andalucia Occidental*. Seville: Universidad de Sevilla, 283–284.

Pau C. 1915. About *Anagallis monelli* L. *Boletín de la Sociedad Aragonesa de Ciencias Naturales* **14:** 100–107.

Petit C, **Bretagnolle F**, **Felber F. 1999.** Evolutionary consequences of diploid–polyploid hybrid zones in wild species. *Trends in Ecology & Evolution* **14:** 306–311.

Postigo Mijarra JM, **Barrón E**, **Gómez Manzaneque F**, **Morla C. 2009.** Floristic changes in the Iberian Peninsula and Balearic Islands (south-west Europe) during the Cenozoic. *Journal of Biogeography* **36:** 2025–2043.

Puillandre N, **Lambert A**, **Brouillet S**, **Achaz G. 2012.** ABGD, automatic barcode gap discovery for primary species delimitation. *Molecular Ecology* **21:** 1864–1877.

Pujadas A. 1997. *Anagallis* L. In: Castroviejo S, Aedo C, Laínz M, Morales R, Muñoz Garmendia F, Nieto Feliner G, Paiva J. eds. *Flora iberica, V. Ebenaceae-Saxifragaceae*. Madrid: Real Jardín Botánico, CSIC, 57–62.

Quintana A, **Freyre R**, **Davis TM**, **Griesbach RJ. 2008.** Genetic studies of flower color in *Anagallis monelli* L. *HortScience* **43:** 1680–1685.

Rambaut A, **Drummond AJ**, **Xie D**, **Baele G**, **Suchard MA. 2018.** Posterior summarization in Bayesian phylogenetics using Tracer 1.7. *Systematic Biology* **67:** 901–904.

Rausher MD. 2008. Evolutionary transitions in floral color. *International Journal of Plant Sciences* **169:** 7–21.

Revell LJ. 2012. Phytools: an R package for phylogenetic comparative biology (and other things). *Methods in Ecology and Evolution* **3:** 217–223.

Rieseberg LH, **Raymond O**, **Rosenthal DM**, **Lai Z**, **Livingstone K**, **Nakazato T**, **Durphy JL**, **Schwarzbach AE**, **Donovan LA**, **Lexer C. 2003.** Major ecological transitions in wild sunflowers facilitated by hybridization. *Science* **301:** 1211–1216.

Rodríguez-Sánchez F, **Pérez-Barrales R**, **Ojeda F**, **Vargas P**, **Arroyo J. 2008.** The Strait of Gibraltar as a melting pot for plant biodiversity. *Quaternary Science Reviews* **27:** 2100–2117.

Rodrigo A, **Bertels F**, **Heled J**, **Noder R**, **Shearman H**, **Tsai P. 2008.** The perils of plenty: what are we going to do with all these genes? *Philosophical Transactions of the Royal Society B: Biological Sciences* **363:** 3893–3902.

Ronquist F, **Teslenko M**, **van der Mark P**, **Ayres DL**, **Darling A**, **Höhna S**, **Larget B**, **Liu L**, **Suchard MA**, **Huelsenbeck JP. 2012.** MrBayes 3.2: efficient Bayesian phylogenetic inference and model choice across a large model space. *Systematic Biology* **61:** 539–542.

Rosenberg NA. 2007. Statistical tests for taxonomic distinctiveness from observations of monophyly. *Evolution* **61:** 317–323.

Sampaio G. 1900. Studies on the flora of Porto's surroundings. I. Primulaceae (Vent.) *Annales des Sciences Naturales* **6:** 51–62.

Sánchez-Cabrera M, **Jiménez López FJ**, **Narbona E**, **Arista M**, **Ortiz PL**, **Romero-Campero FJ**, **Ramanauskas K**, **Igic B**, **Fuller AA**, **Whittall JB. 2021.** Changes at a critical branchpoint in the anthocyanin biosynthetic pathway underlie the blue to orange flower color transition in *Lysimachia arvensis*. *Frontiers in Plant Science* **12:** 633979.

Schousboe P. 1800. *Iagttagelser over Vextriget i Marokko. [Observations on the Plant Kingdom in Morocco].* Copenhagen: Forfatteren hos K. H. Seidelin.

Semerikova SA, **Semerikov VL. 2016.** Phylogeny of firs (genus *Abies*, *Pinaceae*) based on multilocus nuclear markers (AFLP). *Russian Journal of Genetics* **52:** 1164–1175.

Servedio MR, **Van Doorn GS**, **Kopp M**, **Frame AM**, **Nosil P. 2011.** Magic traits in speciation: 'magic' but not rare? *Trends in Ecology & Evolution* **26:** 389.

Shaw J, **Lickey EB**, **Schilling EE**, **Small RL. 2007.** Comparison of whole chloroplast genome sequences to choose noncoding regions for phylogenetic studies in angiosperms: the tortoise and the hare III. *American Journal of Botany* **94:** 275–288.

Sobel JM, **Streisfeld MA. 2015.** Strong premating reproductive isolation drives incipient speciation in *Mimulus aurantiacus*. *Evolution; International Journal of Organic Evolution* **69:** 447–461.

Soltis DE, **Soltis PS. 1998.** Choosing an approach and an appropriate gene for phylogenetic analysis. In Soltis DE, Soltis PS, Doyle JJ, eds. *Molecular systematics of plants II. DNA sequencing*. New York: Springer, 1–42.

Soltis DE, **Visger CJ**, **Soltis PS. 2014.** The polyploidy revolution then…and now: Stebbins revisited. *American Journal of Botany* **101:** 1057–1078.

Soltis PS, **Marchant DB**, **Van de Peer Y**, **Soltis DE. 2015.** Polyploidy and genome evolution in plants. *Current Opinion in Genetics & Development* **35:** 119–125.

Souissi A, **Gagnaire PA**, **Bonhomme F**, **Bahri-Sfar L. 2017.** Introgressive hybridization and morphological transgression in the contact zone between two Mediterranean *Solea* species. *Ecology and Evolution* **7:** 1394–1402.

Stamatakis A. 2014. RAxML version 8: a tool for phylogenetic analysis and post-analysis of large phylogenies. *Bioinformatics (Oxford, England)* **30:** 1312–1313.

Stecher G, **Tamura K**, **Kumar S. 2020.** Molecular evolutionary genetics analysis (MEGA) for macOS. *Molecular Biology and Evolution* **37:** 1237–1239.

Strauss SY, **Whittall JB. 2006.** Non-pollinator agents of selection on floral traits. In: Harder LD, Barrett SCH, eds. *Ecology and evolution of flowers*. Oxford: Oxford University Press, 120–138.

Suc JP. 1984. Origin and evolution of the Mediterranean vegetation and climate in Europe. *Nature* **307:** 429–432.

Suchard MA, **Lemey P**, **Baele G**, **Ayres DL**, **Drummond AJ**, **Rambaut A. 2018.** Bayesian phylogenetic and phylodynamic data integration using BEAST 1.10. *Virus Evolution* **4:** vey016.

Šveřepová G. 1972. On the cytotaxonomy of the genus *Anagallis* L. (K cytotaxonomi rodu *Anagallis* L.). *Preslia* **44:** 219–226.

Swofford DL. 2003. *PAUP*. Phylogenetic analysis using parsimony (*and other methods), Version 4*. Sunderland: Sinauer Associates.

Symonds VV, **Lloyd AM. 2003.** An analysis of microsatellite loci in *Arabidopsis thaliana*: mutational dynamics and application. *Genetics* **165:** 1475–1488.

Takahashi Y, **Takakura KI**, **Kawata M. 2016.** Spatial distribution of flower color induced by interspecific sexual interaction. *PLoS One* **11:** e0164381.

Talavera S, **Gibbs PE**, **Fernández-Piedra MP**, **Ortiz-Herrera MA. 2001.** Genetic control of self-incompatibility in *Anagallis monelli* (Primulaceae: Myrsinaceae). *Heredity* **87:** 589–597.

Thompson JD, **Gibson T**, **Higgins DG. 2002.** Multiple sequence alignment using ClustalW and ClustalX. *Current Protocols in Bioinformatics* **1:** 2–3.

Tournefort JP. 1719. *Instituciones rei herbariae*, 3rd edn, **Vol. 1**. Paris: Typographia Regia.

Valdés B. 1970. Números cromosómicos de algunas plantas españolas. *Boletin de la Real Sociedad Española de Historia Natural (Biología)* **68:** 193–197.

Vargas P. 2003. Molecular evidence for multiple diversification patterns of alpine plants in Mediterranean Europe. *Taxon* **52:** 463–476.

Viruel J, **Forest F**, **Paun O**, **Chase MW**, **Devey D**, **Couto RS**, **Segarra-Moragues JG**, **Catalán P**, **Wilkin P. 2018.** A nuclear *Xdh* phylogenetic analysis of yams (*Dioscorea*: Dioscoreaceae) congruent with plastid trees reveals a new Neotropical lineage. *Botanical Journal of the Linnean Society* **187:** 232–246.

Viruel J, **Segarra-Moragues JG**, **Raz L**, **Forest F**, **Wilkin P**, **Sanmartín I**, **Catalán P. 2016.** Late Cretaceous–Early Eocene origin of yams (*Dioscorea*, Dioscoreaceae) in the Laurasian Palaearctic and their subsequent Oligocene–Miocene diversification. *Journal of Biogeography* **43:** 750–762.

Volkov R, **Borisjuk ANV**, **Panchuk II**, **Schweizer D**, **Hemleben V. 1999.** Elimination and rearrangement of parental rDNA in the allotetraploid *Nicotiana tabacum*. *Molecular Biology and Evolution* **16:** 311–320.

Wakeley J. 2009. *Coalescent theory: an introduction*. Greenwood Village: Roberts and Company Publishers.

Wang H, **Conchou L**, **Bessière JM**, **Cazals G**, **Schatz B**, **Imbert E. 2013.** Flower color polymorphism in *Iris lutescens* (Iridaceae): biochemical analyses in light of plant–insect interactions. *Phytochemistry* **94:** 123–134.

Wang J, **Tian L**, **Lee HS**, **Chen ZJ. 2006.** Nonadditive regulation of FRI and FLC loci mediates flowering-time variation in *Arabidopsis* allopolyploids. *Genetics* **173:** 965–974.

Wendel JF, **Doyle JJ. 1998.** Phylogenetic incongruence: window into genome history and molecular evolution. In: Soltis DE, Soltis PS, Doyle JJ, eds. *Molecular systematics of plants II. DNA sequencing*. New York: Springer, 265–296.

Wessinger CA, **Rausher MD. 2012.** Lessons from flower colour evolution on targets of selection. *Journal of Experimental Botany* **63:** 5741–5749.

White TJ, **Bruns T**, **Lee S**, **Taylor J. 1990.** Amplification and direct sequencing of fungal ribosomal RNA genes for phylogenetics. In: Innis MA, Gelfand DH, Sninsky JJ, White TJ, eds. *PCR protocols: a guide to methods and applications*. New York: Academic Press, 315–322.

Wickham H. 2011. ggplot2. *Wiley Interdisciplinary Reviews: Computational Statistics* **3:** 180–85.

Willkomm HM. 1870. Primulaceae. In: Willkomm HM, Lange JM, eds. *Prodromus Florae Hispanicae, 2*. Stuttgart: E. Schweizerbart (E. Koch), 635–650.

Wilson P, **Wolfe AD**, **Armbruster WS**, **Thomson JD. 2007.** Constrained lability in floral evolution: counting convergent origins of hummingbird pollination in *Penstemon* and *Keckiella*. *The New Phytologist* **176:** 883–890.

Wood TE, **Takebayashi N**, **Barker MS**, **Mayrose I**, **Greenspoon PB**, **Rieseberg LH. 2009.** The frequency of polyploid speciation in vascular plants. *Proceedings of the National Academy of Sciences USA* **106:** 13875–13879.

Yan HF, **Zhang CY**, **Anderberg AA**, **Hao G**, **Ge XJ**, **Wiens JJ. 2018.** What explains high plant richness in East Asia? Time and diversification in the tribe Lysimachieae (Primulaceae). *The New Phytologist* **219:** 436–448.

Yesson C, **Toomey NH**, **Culham A. 2009.** *Cyclamen*: time, sea and speciation biogeography using a temporally calibrated phylogeny. *Journal of Biogeography* **36:** 1234–1252.

Zanne AE, **Tank DC**, **Cornwell WK**, **Eastman JM**, **Smith SA**, **FitzJohn RG**, **McGlinn DJ**, **O'Meara BC**, **Moles AT**, **Reich PB**, **Royer DL**, **Soltis DE**, **Stevens PF**, **Westoby M**, **Wright IJ**, **Aarssen L**, **Bertin RI**, **Calaminus A**, **Govaerts R**, **Hemmings F**, **Leishman MR**, **Oleksyn J**, **Soltis PS**, **Swenson NG**, **Warman L**, **Beaulieu JM. 2014.** Three keys to the radiation of angiosperms into freezing environments. *Nature* **506:** 89–92.

SUPPORTING INFORMATION

Additional Supporting Information may be found in the online version of this article at the publisher's web-site:

Figure S1. Maximum clade credibility tree based on ITS sequences including a recombinant sample of *Lysimachia arvensis* (LA19_B).
Figure S2. Phylogenetic network and maximum-likelihood tree of *Lysimachia* based on *rps16-trnK* plastid sequence data.
Figure S3. Phylogenetic network and maximum-likelihood tree of *Lysimachia* based on *rpl32-trnL* plastid sequence data.
Figure S4. Phylogenetic network and maximum-likelihood tree of *Lysimachia* based on *psbA-trnH* plastid sequence data.
Figure S4. Maximum clade credibility tree based on three combined plastid sequences dataset.
Figure S6. Frequency distributions of pairwise Kimura two-parameter distances.
Figure S7. Maximum clade credibility tree of tribe Lysimachieae.
Table S1. Population information of samples.
Table S2. Condition and information of primer combinations tested.
Table S3. GenBank accession numbers of sequences of tribe Lysimachieae used.
Table S4. Divergence times of major clades based on different tree priors (Yule, birth–death) and calibration points.
Table S5. Regression results between the node ages of all clades from the primary tree and the alternative trees.